6-11-2024

Nucleation Control System and Method Leading to Enhanced Boiling Based on Electric Cooling

Amitabh Narain
Michigan Technological University, narain@mtu.edu

Soroush Sepahyar

Divya Kamlesh Pandya

Vibhu Vivek

US012010816B2

(12) **United States Patent**
Narain et al.

(10) **Patent No.: US 12,010,816 B2**
(45) **Date of Patent: Jun. 11, 2024**

(54) **NUCLEATION CONTROL SYSTEM AND METHOD LEADING TO ENHANCED BOILING BASED ELECTRONIC COOLING**

(71) Applicant: **MICHIGAN TECHNOLOGICAL UNIVERSITY**, Houghton, MI (US)

(72) Inventors: **Amitabh Narain**, Houghton, MI (US); **Soroush Sepahyar**, Hancock, MI (US); **Divya Kamlesh Pandya**, Houghton, MI (US); **Vibhu Vivek**, Santa Clara, CA (US)

(73) Assignee: **MICHIGAN TECHNOLOGICAL UNIVERSITY**, Houghton, MI (US)

(*) Notice: Subject to any disclaimer, the term of this patent is extended or adjusted under 35 U.S.C. 154(b) by 208 days.

(21) Appl. No.: **17/291,728**

(22) PCT Filed: **Nov. 12, 2019**

(86) PCT No.: **PCT/US2019/060994**
§ 371 (c)(1),
(2) Date: **May 6, 2021**

(87) PCT Pub. No.: **WO2020/102239**
PCT Pub. Date: **May 22, 2020**

(65) **Prior Publication Data**

US 2022/0015266 A1 Jan. 13, 2022

Related U.S. Application Data

(60) Provisional application No. 62/870,624, filed on Jul. 3, 2019, provisional application No. 62/833,551, filed
(Continued)

(51) **Int. Cl.**
H05K 7/20 (2006.01)
F28D 15/02 (2006.01)
(Continued)

(52) **U.S. Cl.**
CPC ***H05K 7/20327*** (2013.01); ***F28D 15/0233*** (2013.01); ***F28D 15/046*** (2013.01);
(Continued)

(58) **Field of Classification Search**
CPC F28F 13/185; F28F 13/187; F28F 13/10; F28F 2260/02; H01L 23/427; H05K 7/20309; F28D 15/046; F28D 15/0233
See application file for complete search history.

(56) **References Cited**

U.S. PATENT DOCUMENTS

7,238,085 B2 7/2007 Montierth et al.
7,261,144 B2 8/2007 Thome et al.
(Continued)

FOREIGN PATENT DOCUMENTS

WO WO-2014047338 A1 * 3/2014 ..... F28F 13/10
WO WO2014047338 A1 3/2014

OTHER PUBLICATIONS

Agarwal et al., "Principle and applications of microbubble and nanobubble technology for water treatment" Chemosphere 84, No. 9 (2011): pp. 1175-1180.
(Continued)

Primary Examiner — Tavia Sullens
Assistant Examiner — Khaled Ahmed Ali Al Samiri
(74) *Attorney, Agent, or Firm* — Michael Best & Friedrich LLP

(57) **ABSTRACT**

A cooling module for an electronic device includes a body having formed therein a plurality of channels, a micro-structured boiling surface, a piezoelectric transducer, an inlet header, and an outlet header. Each channel of the plurality of channels is defined by a first channel surface and opposing lateral channel surfaces cooperatively defining a rectangular cross section normal to a channel axis. The micro-structured boiling surface is positioned adjacent the
(Continued)

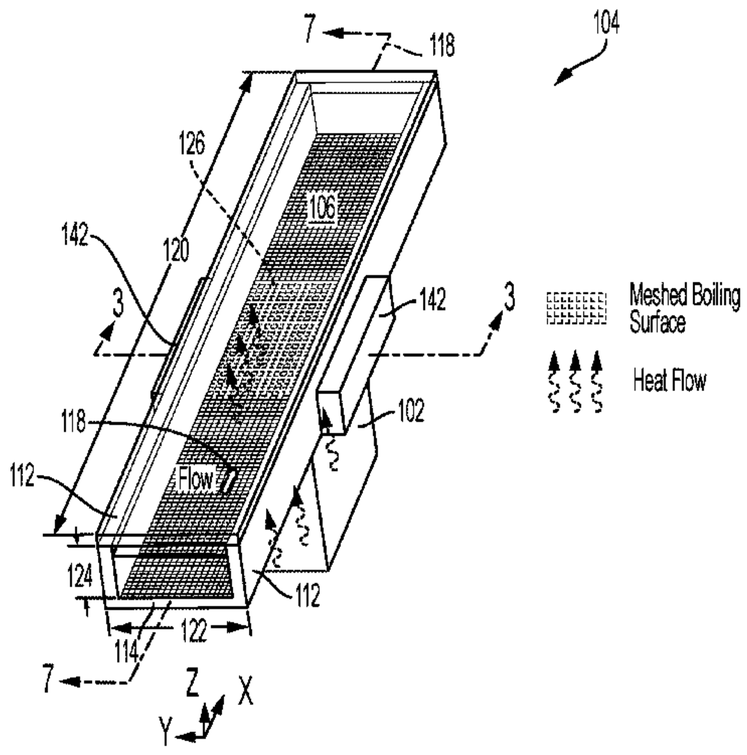

first channel surface of each channel. The piezoelectric transducer is in acoustic communication with one of the opposing lateral channel surfaces of each channel and configured to direct acoustic waves on the micro-structured boiling surface. The inlet header is in fluid communication with each channel of the plurality of channels. The outlet header is in fluid communication with each channel of the plurality of channels.

11 Claims, 20 Drawing Sheets

Related U.S. Application Data

on Apr. 12, 2019, provisional application No. 62/759,961, filed on Nov. 12, 2018.

(51) **Int. Cl.**
F28D 15/04 (2006.01)
F28F 13/10 (2006.01)

(52) **U.S. Cl.**
CPC ***F28F 13/10*** (2013.01); ***H05K 7/20309*** (2013.01); *F28F 2260/02* (2013.01)

(56) **References Cited**

U.S. PATENT DOCUMENTS

7,730,605	B2 *	6/2010	Yeh	F28D 15/0233 29/613
8,051,905	B2 *	11/2011	Arik	H01L 23/4735 239/102.1
9,103,468	B2	8/2015	Li et al.	
9,207,025	B2	12/2015	Varanasi et al.	
9,327,317	B2 *	5/2016	Hynynen	H10N 30/875
9,603,284	B2	3/2017	Lyon	
2006/0137856	A1	6/2006	Popovich	
2007/0023169	A1	2/2007	Mahalingam et al.	
2013/0025831	A1	1/2013	Attinger et al.	
2016/0054031	A1	2/2016	Echart et al.	
2017/0176114	A1	6/2017	Kandlikar et al.	
2017/0299239	A1	10/2017	Steven	

OTHER PUBLICATIONS

Aquila Group, Aquiarius Water Cooled Computing Solutions, Fixed-plate Liquid-cooling solution: webpage: https://www.aquilagroup.com/cooling/, Copyright 2022, (8 Pages).
Asetek, "Passion. Precision. Performance.", website: https://www.asetek.com, Copyright 2021 (5 Pages).
Avgerinou et al., "Trends in data centre energy consumption under the European code of conduct for data centre energy efficiency" Energies 10, (2017): 1470, (18 Pages).
Bar-Cohen et al., "Design and optimization of air-cooled heat sinks for sustainable development", IEEE transactions on components and packaging technologies 25, No. 4, (2002): pp. 584-591.
Bigham et al., "Microscale study of mechanisms of heat transfer during flow boiling in a microchannel" International Journal of Heat and Mass Transfer 88 (2015): pp. 111-121.
Campbell, Steve. "Is Liquid Cooling Ready to Go Mainstream?" URL: https://www.hpcwire.com/2017/02/13/liquid-cooling-ready-go-mainstream, Feb. 13, 2017 (6 Pages).
Carey VP, "Liquid-vapor phase-change phenomena. Series in chemical and mechanical engineering", Hemisphere Publishing Corporation, New York (1992), (5 Pages—Table of Contents of Book).
Chainer et al., "Improving Data Center Energy Efficiency with Advanced Thermal Management", IEEE Transactions on Components, Packaging and Manufacturing Technology (2017), pp. 1228-1239.
Chien et al., "A nucleate boiling model for structured enhanced surfaces", International Journal of Heat and Mass Transfer 41, No. 14 (1998), pp. 2183-2195.
Chu et al., "Structured surfaces for enhanced pool boiling heat transfer", Applied Physics Letters 100, No. 24 (2012): 241603, (5 Pages).
Chu et al., "Hierarchically structured surfaces for boiling critical heat flux enhancement", Applied Physics Letters 102, No. 15 (2013): 151602, (5 Pages).
Coolit Systems, "771-00012 rev A18 Rack DCLC Product Guide," URL, https://ww1.prweb.com/prfiles/2018/11/11/15910148/771-00012%20rev%20A18_NEW%20CoollT%20Rack%20DCLC%20Product%20Guide.pdf, first accessed at least as early as Jul. 5, 2019, (16 Pages).
Del Valle et al., "Subcooled flow boiling at high heat flux", International Journal of Heat and Mass Transfer 28, No. 10 (1985): pp. 1907-1920.
Dong et al. "An experimental investigation of enhanced pool boiling heat transfer from surfaces with micro/nano-structures" International Journal of Heat and Mass Transfer 71 (2014): pp. 189-196.
Douglas et al., "Acoustically Enhanced Boiling Heat Transfer," THERMINIC, Budapest, Hungary, Sep. 17-19, 2007, (5 Pages).
Douglas et al., "Acoustically enhanced boiling heat transfer", Physics of Fluids 24, No. 5 (2012): 052105, (18 Pages).
Fuijitsu, "The Vision of the future with Human-centered technology" website: http://www.fujitsu.com/global/, Copyright 1995 (7 Pages).
Gerardi et al., "Infrared thermometry study of nanofluid pool boiling phenomena", Nanoscale research letters 6, No. 1 (2011): 232, (17 Pages).
Ghiaasiaan, S.M., "Two-phase flow, boiling, and condensation: in conventional and miniature systems", Cambridge University Press, Cambridge, (2007), (8 Pages—Table of Contents of Book).
Google's Green Data Centers: Network POP Case Study. URL: https://static.googleusercontent.com/media/www.google.com/en//corporate/datacenter/dc-best-practices-google.pdf, 2011, (10 Pages).
Gorgitrattanagul, P., "Experimental investigations of temperature controlled innovative annular flow-boiling of FC-72 in millimeter scale ducts—steady and enhanced pulsatile realizations", Ph. D. Thesis, Michigan Technological University, Dec. 2017, (113 Pages).
Gotovskiy, M. A. et al., "Use of Combines Steam-Water and Organic Rankine Cycles for Achieving Better Efficiency of Gas Turbine Units and Internal Combustion Engines", Thermal Engineering 59, No. 3 (2012): pp. 236-241.
Grebene, H. R. et al., "Phase Locking as a New Approach For Tuned Integrated Circuits", ISSCC Digest of Technical Papers, pp. 100-101, Feb. 1969.
Gupta et al., MS University, "Applied Mechanics; New Applied Mechanics Findings from MS University Discussed, "Vapor Bubble Formation, Forces, and Induced Vibration: A Review, Applied Mechanics Reviews, May 2016, vol. 68, (12 Pages).
Heffington, S et al., "Enhanced boiling heat transfer by submerged ultrasonic vibrations", Therminic Sophia Antipolis, Cote d'Azur (2004), (5 Pages).
Johnsson, Lennart, "Overview of Data Centers Energy Efficiency Evolution. Handbook of Energy Aware and Green Computing, vol. 2, Chap. 43, Ishfaq Ahmad, Sanjay Ranka." (2012). Also: Johnsson, Lennart. "Overview of Data Centers Energy Efficiency Evolution", (2012): pp. 983-1028. Also @ URL: https://pdfs.semanticscholar.org/559f/5b4bb297999ed00d4a787cf9317ec515afa1.pdf.
Kandlikar, Satish G., "Heat transfer mechanisms during flow boiling in microchannels", In ASME 2003 1st International Conference on Microchannels and Minichannels, pp. 33-46. American Society of Mechanical Engineers, 2003.
Karpelson, Michael, et al., "Driving high voltage piezoelectric actuators in microrobotic applications", Sensors and actuators A: Physical 176 (2012): pp. 78-89.
Kim, Jungho, "Spray cooling heat transfer: the state of the art", International Journal of Heat and Fluid Flow 28, No. 4 (2007): pp. 753-767.
Kim et al., "Surface wettability change during pool boiling of nanofluids and its effect on critical heat flux", International Journal of Heat and Mass Transfer 50, No. 19-20 (2007): pp. 4105-4116.

(56) **References Cited**

OTHER PUBLICATIONS

Kivisalu et al., "Results for High Heat-Flux Flow Realizations in Innovative Operations of Milli-Meter Scale Condensers and Boilers", International Journal of Heat and Mass Transfer. 2014, 75, (2014), pp. 381-398.
Koomey, Jonathan, "Growth in data center electricity use 2005 to 2010", A report by Analytical Press, completed at the request of The New York Times 9 (2011), (24 Pages).
Kunkelmann et al., "The effect of three-phase contact line speed on local evaporative heat transfer: Experimental and numerical investigations", International Journal of Heat and Mass Transfer, (2012), 55 (7-8): pp. 1896-1904.
Kuo et al., "Bubble dynamics during boiling in enhanced surface microchannels" Journal of Microelectromechanical Systems 15, No. 6 (2006): pp. 1514-1527.
Legay et al., "Enhancement of heat transfer by ultrasound: review and recent advances", International Journal of Chemical Engineering, (2011), (18 Pages).
Li et al., "Nanostructured copper interfaces for enhanced boiling" small 4, No. 8 (2008): pp. 1084-1088.
Marcinichen et al., "Dynamic flow control and performance comparison of different concepts of two-phase on-chip cooling cycles", Applied Energy 114 (2014): pp. 179-191.
McCarthy et al., "Materials, fabrication, and manufacturing of micro/nanostructured surfaces for phase-change heat transfer enhancement", Nanoscale and Microscale Thermophysical Engineering 18, No. 3 (2014): pp. 288-310.
Mchale et al., "Bubble nucleation characteristics in pool boiling of a wetting liquid on smooth and rough surfaces.", International Journal of Multiphase Flow, 36 (4), (2010): pp. 249-260.
Moghaddam et al., "Physical mechanisms of heat transfer during single bubble nucleate boiling of FC-72 under saturation conditions-I Experimental investigation", International Journal of Heat and Mass Transfer 52, No. 5-6 (2009): pp. 1284-1294.
Mouton, The Unveiling of a Revolutionary New Liquid Cooling Technology, Jun. 2, 2016, (5 Pages).
Narain et al., "Significant Enhancements in Data Center Cooling Rates (or Power Density) Along with Associated Waste Heat Recovery as Electricity," ASME ES 2019—3967, 13th International Conference on Energy Sustainability Bellevue, WA, Jul. 14-17, 2019, (27 Pages).
Narain et al., "Internal Annular Flow Condensation and Flow Boiling: Context, Results, and Recommendations", In: Kulacki FA (ed.) Handbook of Thermal Science and Engineering, 2018, vol. 3, pp. 2075-2162, Springer, Cham. Invited Article.
Ohta et al., "Experimental investigation on observed scattering in heat transfer characteristics for flow boiling in a small diameter tube." Heat transfer engineering 30, No. 1-2 (2009): pp. 19-27.
Parida et al., "Experimental investigation of water cooled server microprocessors and memory devices in an energy efficient chillerless data center", In Semiconductor Thermal Measurement and Management Symposium (SEMI-THERM), 2012 28th Annual IEEE, pp. 224-231.
Radek et al., "Efficient surfaces for boiling heat transfer enhancement", Czasopismo Techniczne 2016, No. Mechanika Zeszyt 4-M, (2016): pp. 3-8.
Schmidt et al., "Experimental Study of the Effects of an Ultrasonic Field in a Nucleate Boiling System," J. Heat Transfer, (1967), 89(4):, pp. 289-294.
Sepahyar, "Influence of Micro-nucleate Boiling on Annular Flow Regime Heat Transfer Coefficient Values and Flow Parameters—For High Heat-Flux Flow Boiling of Water", Ph. D. Thesis, Michigan Technological University, Dec. 2017, (149 Pages).
Shariff, "Enhancement of flow boiling in meso scale channels with subsonic vibrations", J. Micro-Nano Mech. (2009) 5:93-102, (10 Pages).
Shariff, "Acoustics vibrations to enhance flow boiling in micro channels", Int. J. of Thermal & Environmental Engineering 2, No. 1 (2011):, pp. 19-25.
Shinde, MSME from MTU. "Innovative Fin-tubes for a Standard Staggered-bundle Family Leading to Significant Reductions in Air-side Thermal and Pressure-drop Resistances for a Popular Heat-exchanger—Quantitative Characterizations based on a Unique Synthesis of Experiments, Modeling, and Reliable Computations", Fall 2018, (74 Pages).
Tartière et al., "A World Overview of the Organic Rankine Cycle Market", 2017. 129: pp. 2-9.
Tuma, Phillip E, "The merits of open bath immersion cooling of datacom equipment", In Semiconductor Thermal Measurement and Management Symposium, SEMI-THERM 2010. 26th Annual IEEE, pp. 123-131.
Vojini, Amit Dev, MSME from MTU. "Innovative Fin-tubes for a Standard Staggered-bundle Family Leading to Significant Reductions in Air-side Thermal and Pressure-drop Resistances for a Popular Heat-exchanger—Modeling and Analysis in the Context of its Deployment Advantages in the Energy-sector", (Fall 2018), (138 Pages).
Welch et al., "Flexible Combined Cycle Gas Turbine Power Plant Utilising Organic Rankine Cycle Technology" in ASME Turbo Expo 2016: Turbomachinery Technical Conference and Exposition, American Society of Mechanical Engineers, (11 Pages).
Wen et al., "Experimental investigation into the pool boiling heat transfer of aqueous based γ-alumina nanofluids", Journal of Nanoparticle Research 7, No. 2-3 (2005): pp. 265-274.
Wilson, J.R., "Electronics Cooling Depends on Innovative Approaches to Thermal Management", Military & Aerospace Electronics, 2009 (26 Pages).
Wirtz et al., "Effect of Flow Bypass on the Performance of Longitudinal Fin Heat Sinks", ASME Journal of Electronic Packaging, 1994, vol. 116, pp. 206-211.
Wu et al. "Experimental evaluation of a controlled hybrid two-phase multi-microchannel cooling and heat recovery system driven by liquid pump and vapor compressor." International Journal of Refrigeration 36, No. 2 (2013): pp. 375-389.
Yadav et al., "Mitigation of Flow Maldistribution in Parallel Microchannel Heat Sink," IEEE Transactions on Components, Packaging and Manufacturing Technology, 2018, In Press—Print ISSN: 2156-3950, Published Online ISSN: 2156-3985.

* cited by examiner

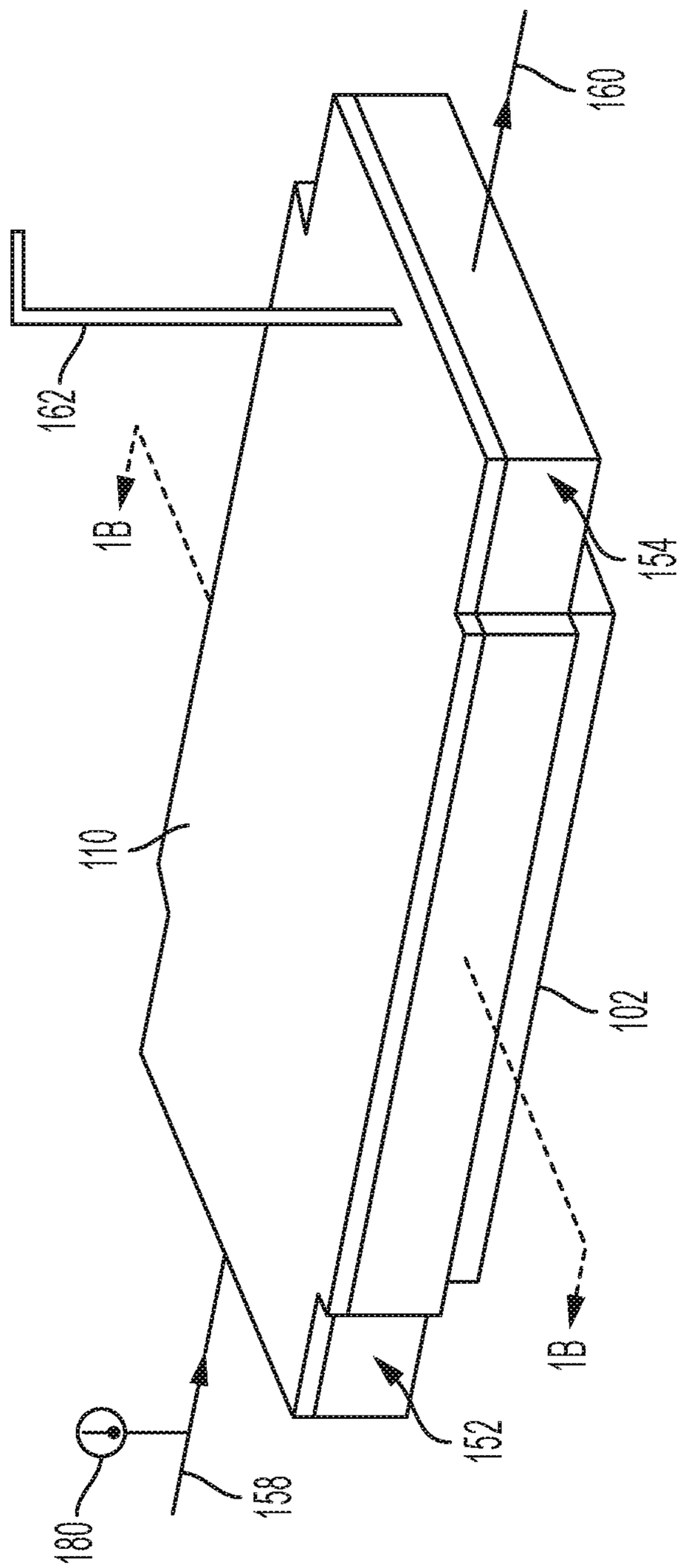

FIG. 1A

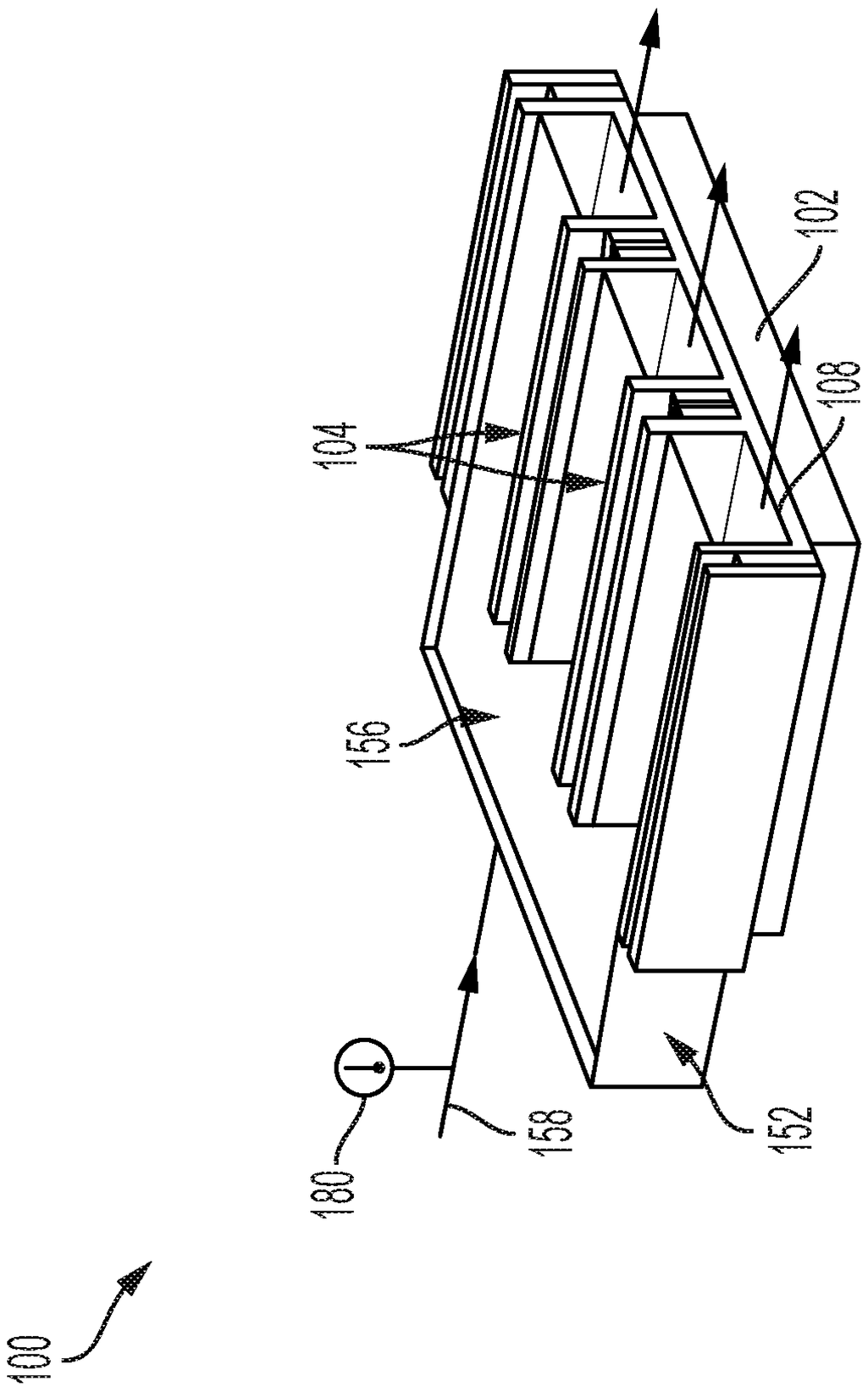

FIG. 1B

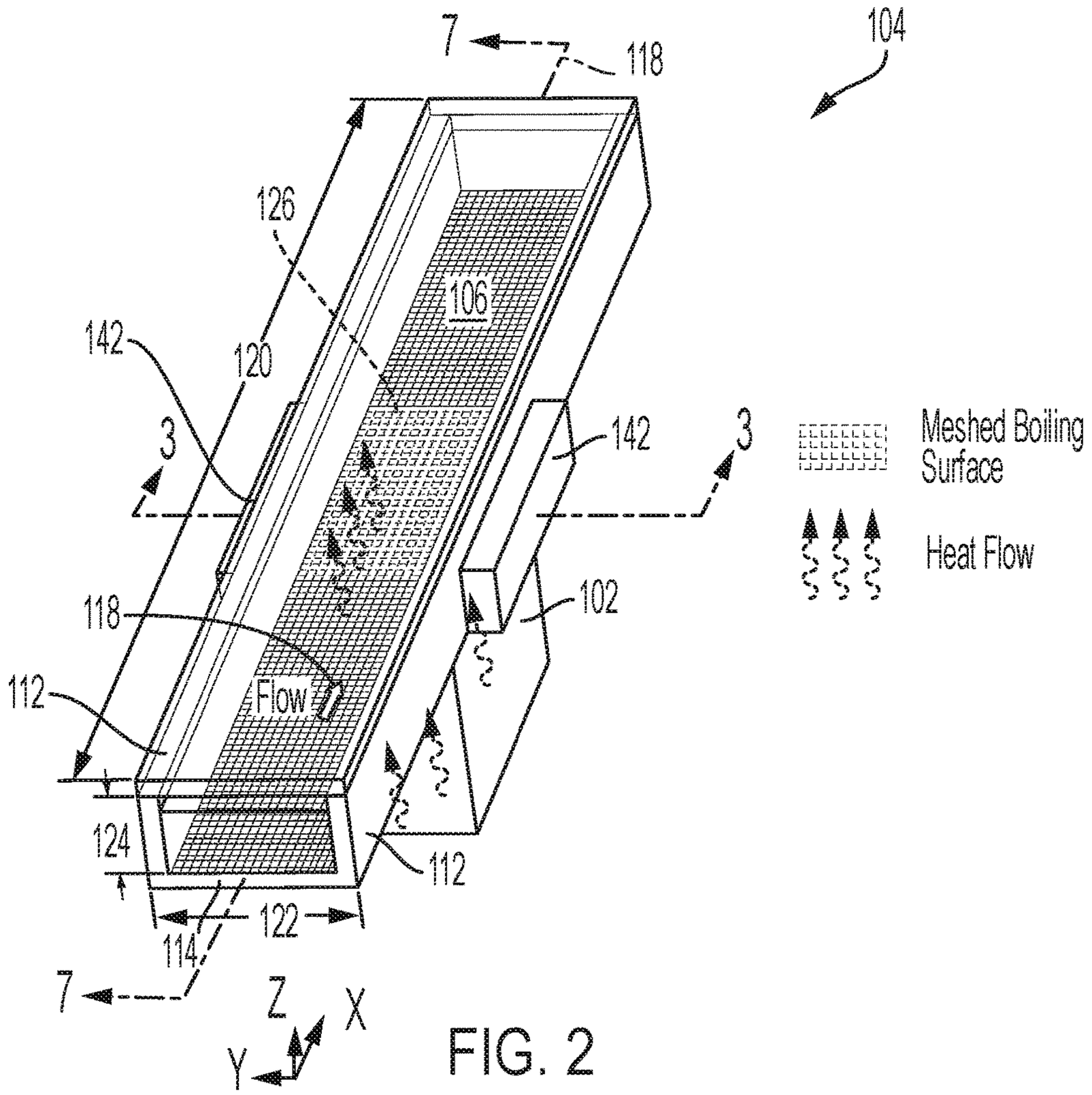

FIG. 2

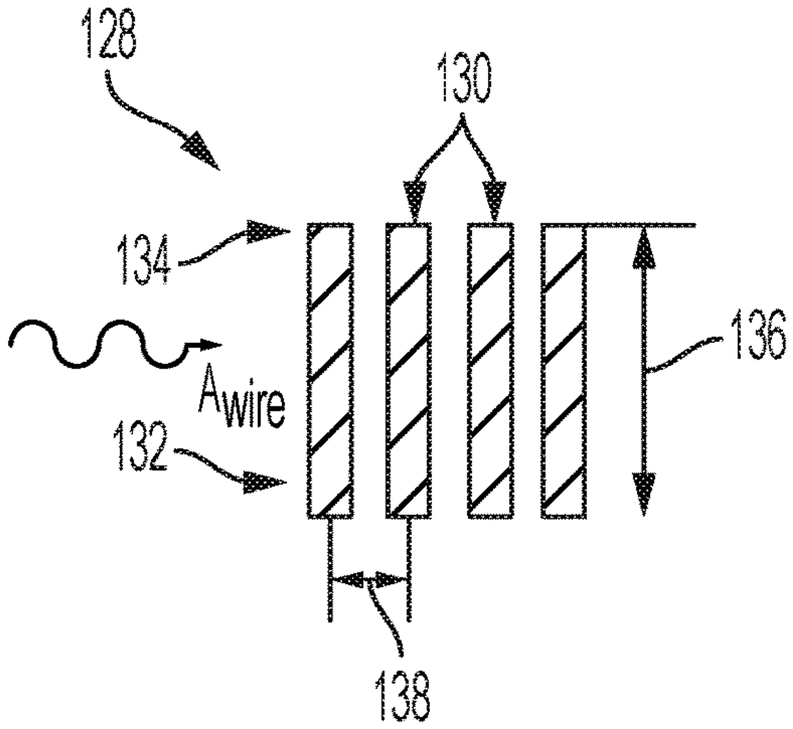

FIG. 3

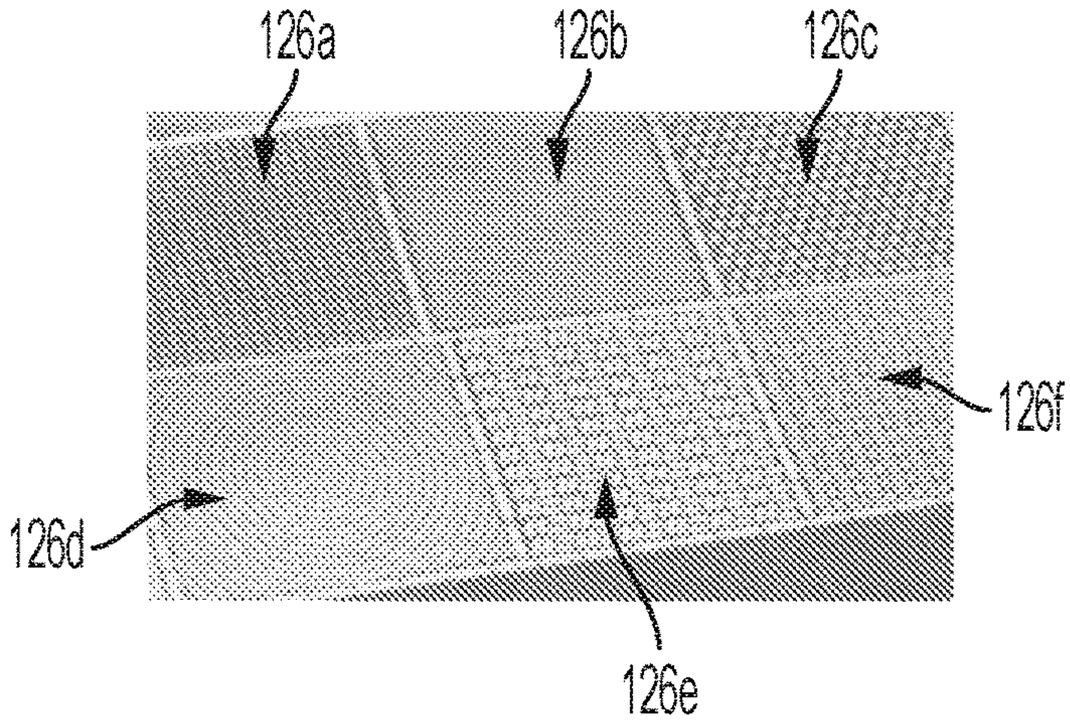

FIG. 4

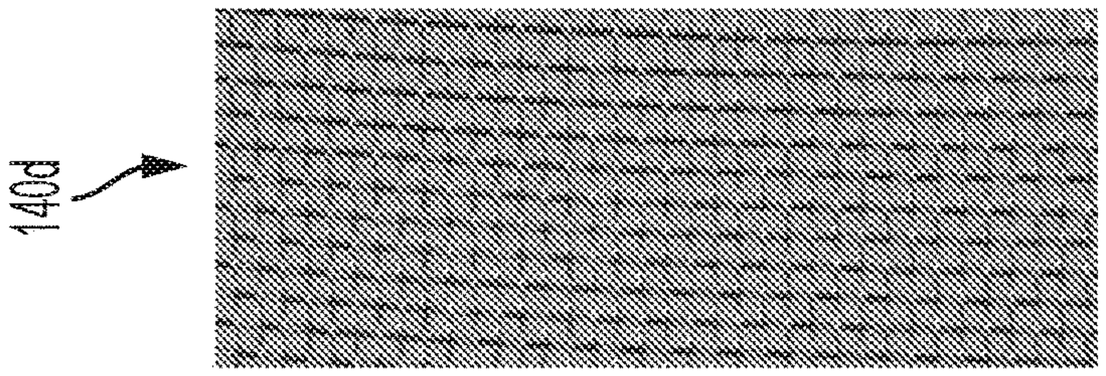

FIG. 5E

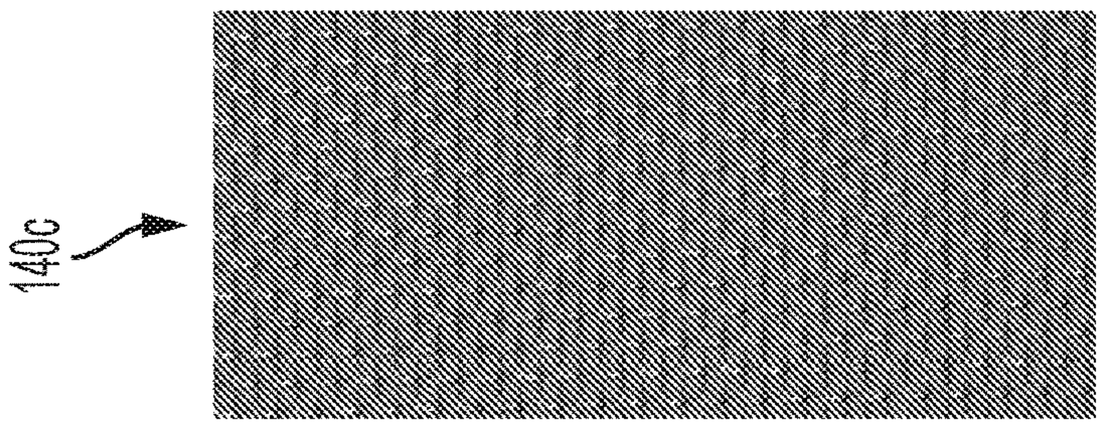

FIG. 5D

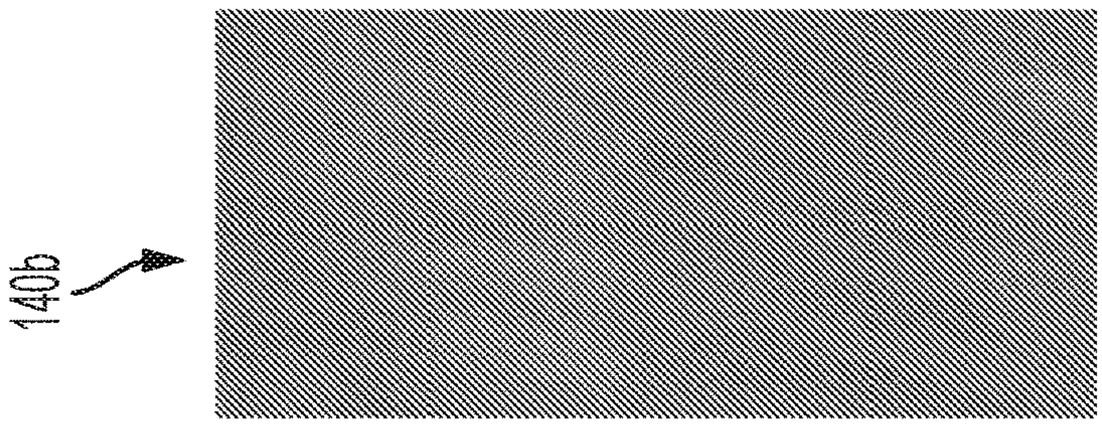

FIG. 5C

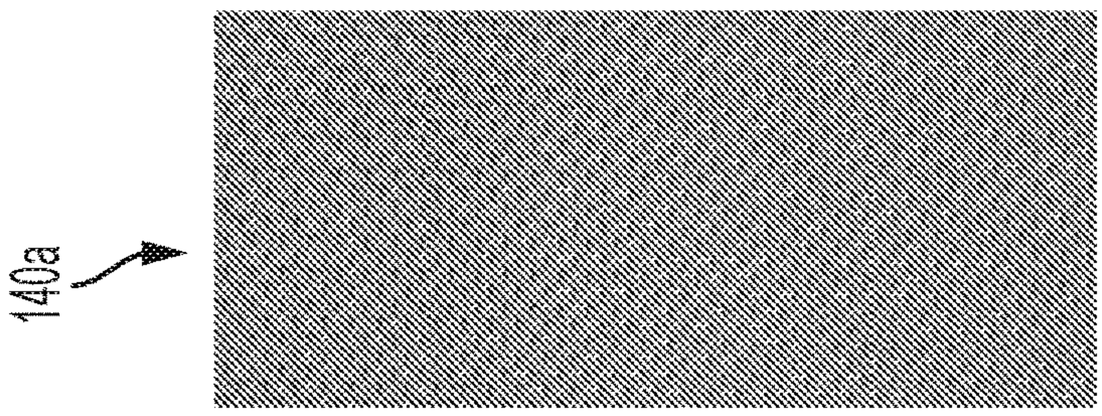

FIG. 5B

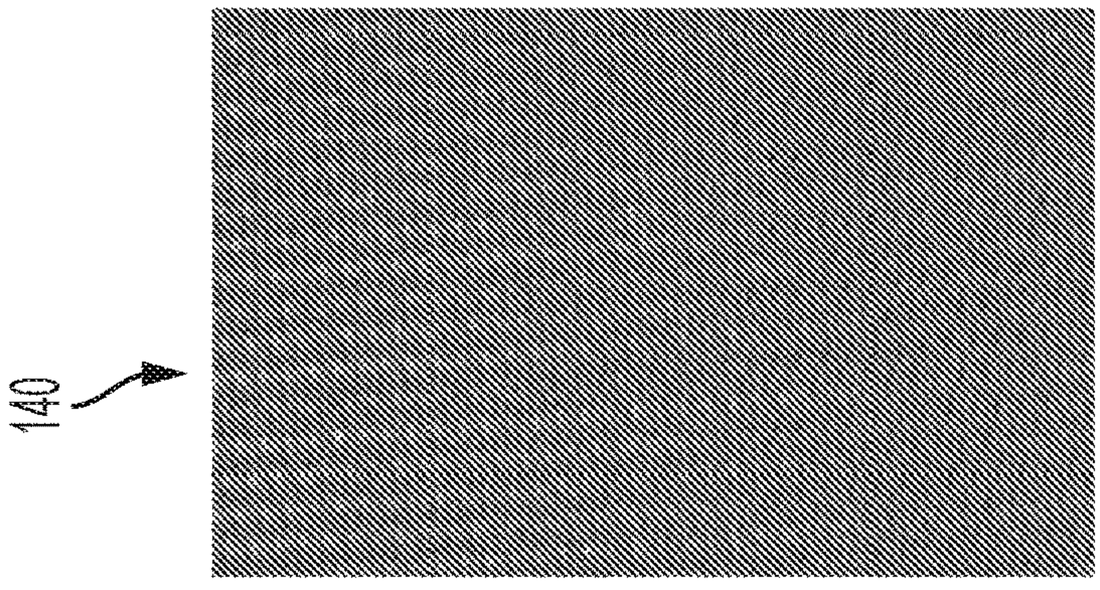

FIG. 5A

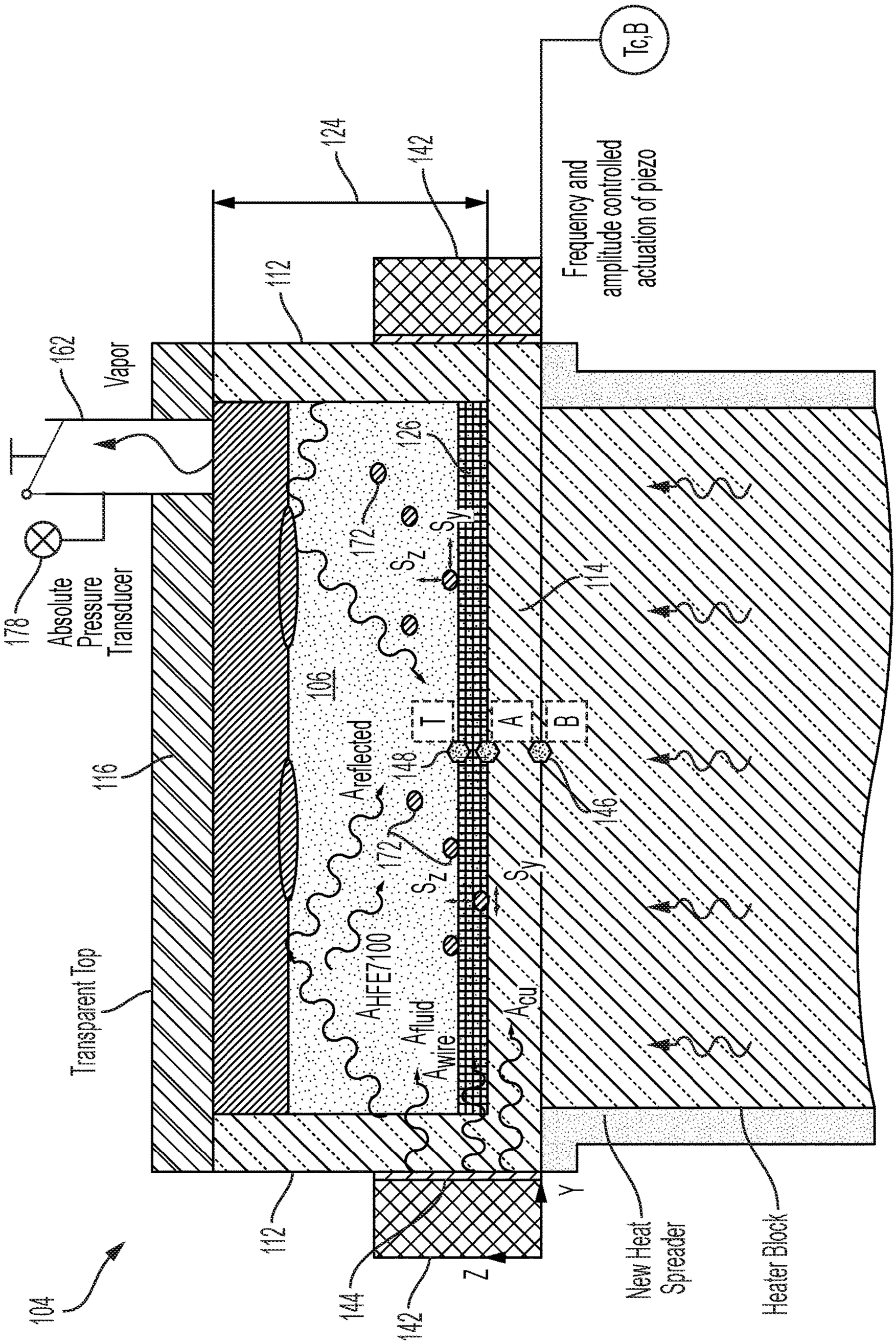
Tc,B
Frequency and amplitude controlled actuation of piezo
124
142
112
162
Vapor
178
Absolute Pressure Transducer
126
172
Sz
Sy
114
106
Areflected
148
T
A
B
116
146
Transparent Top
AHFE7100
Afluid
Awire
Acu
112
144
142
Z
Y
New Heat Spreader
Heater Block
104

FIG. 6

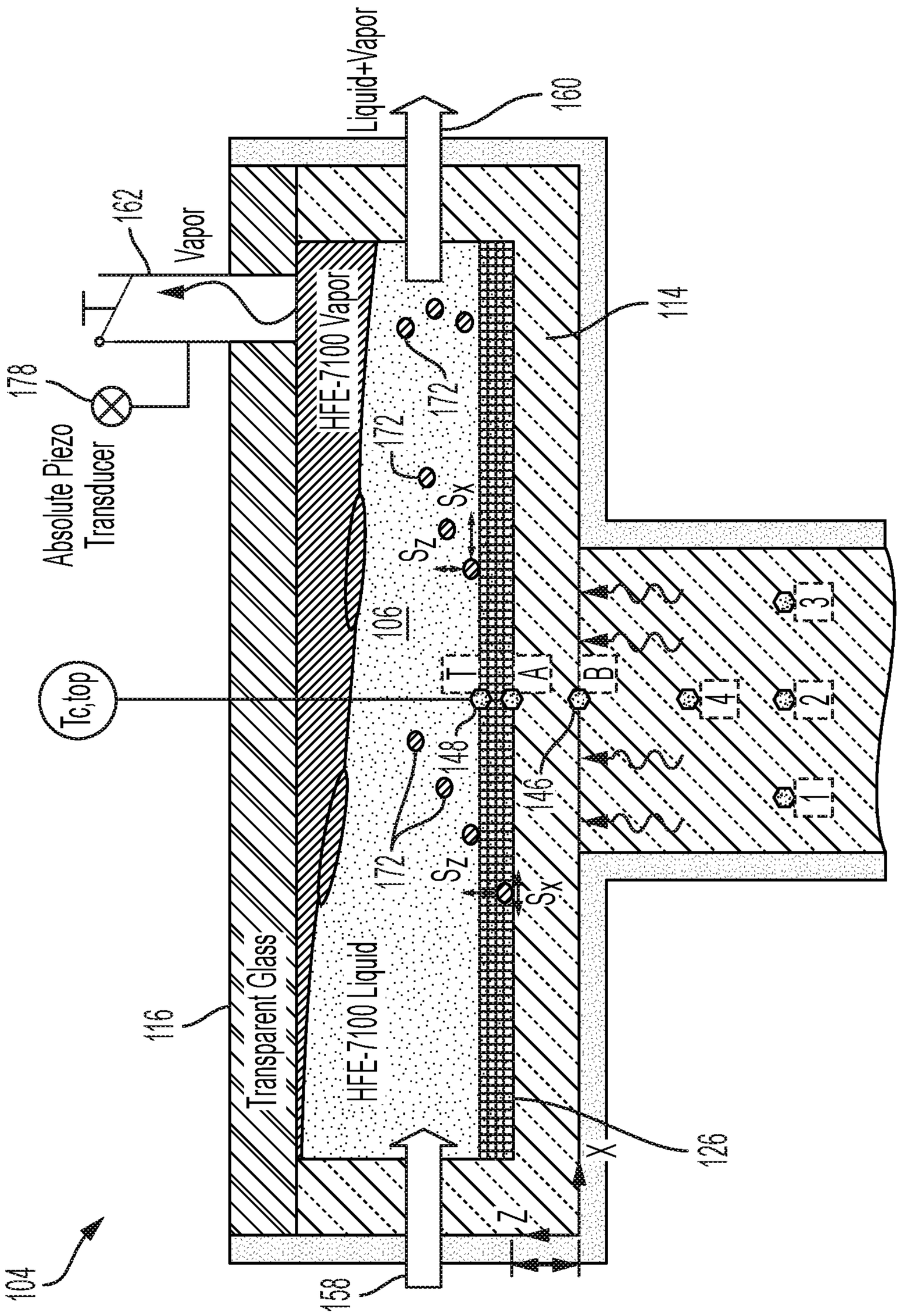
Liquid+Vapor
160
162
Vapor
178
Absolute Piezo Transducer
HFE-7100 Vapor
172
Sz
Sx
106
Tc,top
T
A
B
148
146
114
Heater Block (HB)
1
2
3
4
Transparent Glass
116
HFE-7100 Liquid
Z
X
126
158
104

FIG. 7

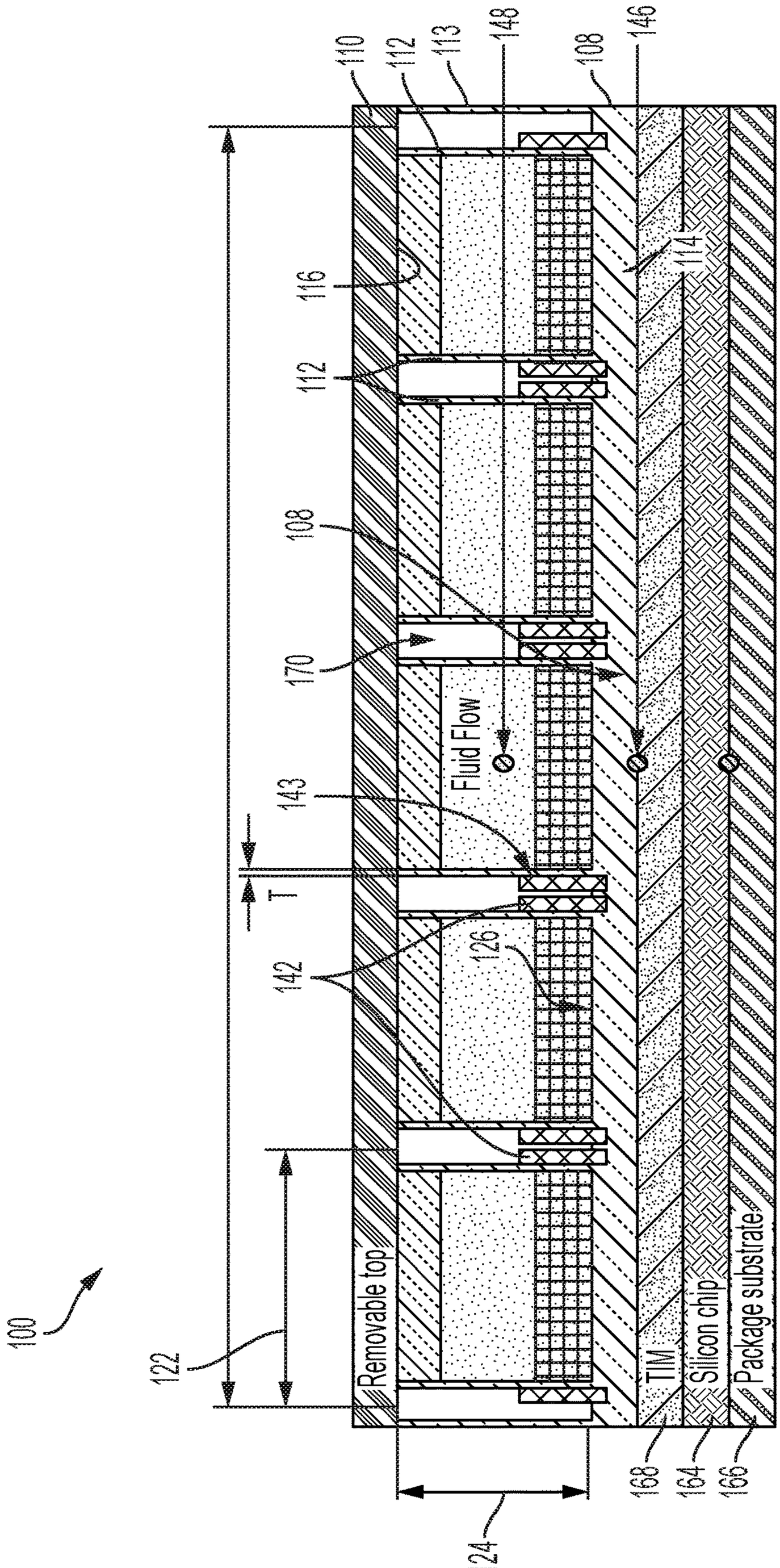
110
112
113
148
108
146
116
114
112
108
170
Fluid Flow
143
T
142
126
122
Removable top
TIM
Silicon chip
Package substrate
168
164
166
124
100

FIG. 8

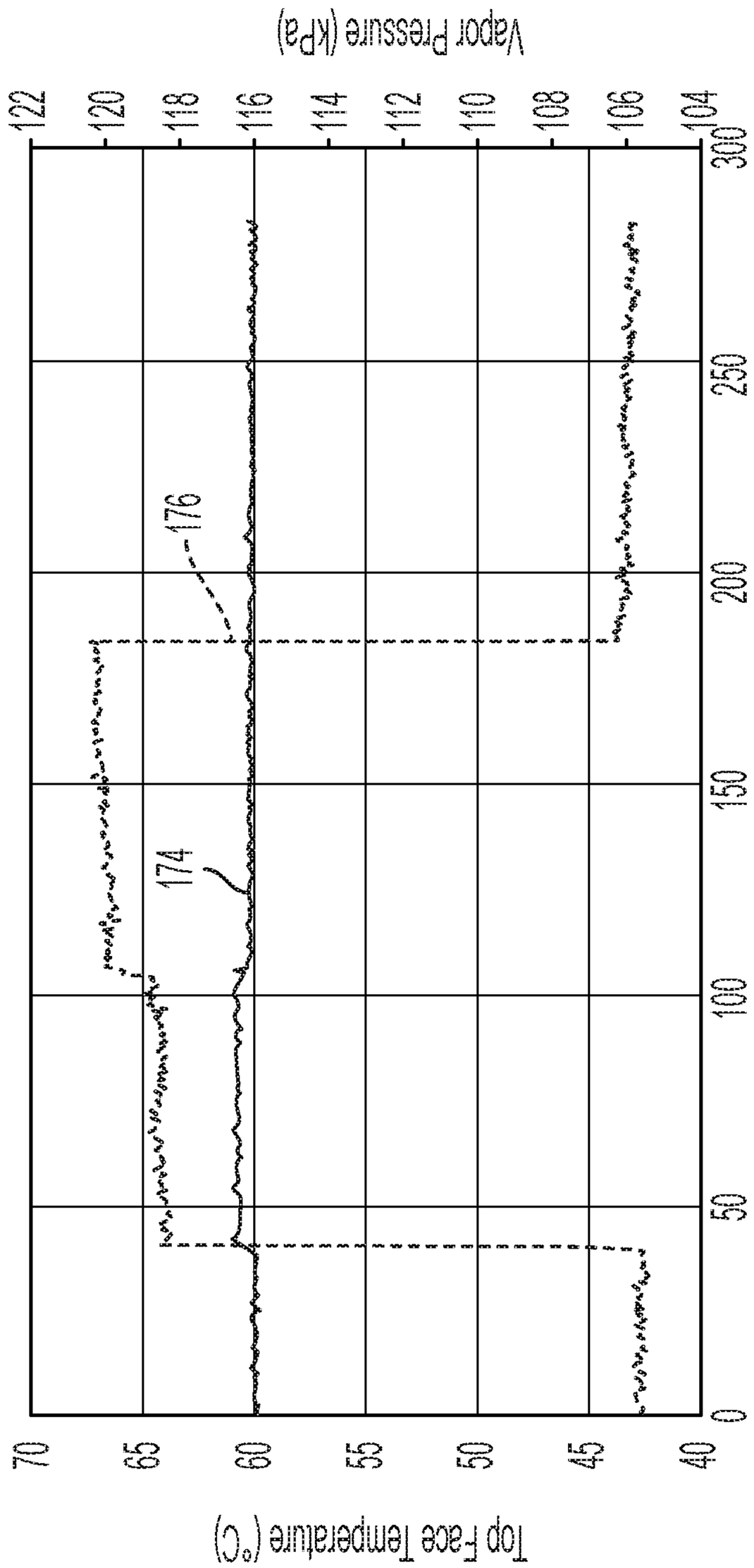
Vapor Pressure (kPa)
122
120
118
116
114
112
110
108
106
104
300
Top Face Temperature
Vapor Pressure
174
176
100
150
200
250
Time (seconds)
0
50
70
65
60
55
50
45
40
Top Face Temperature (°C)

FIG. 9

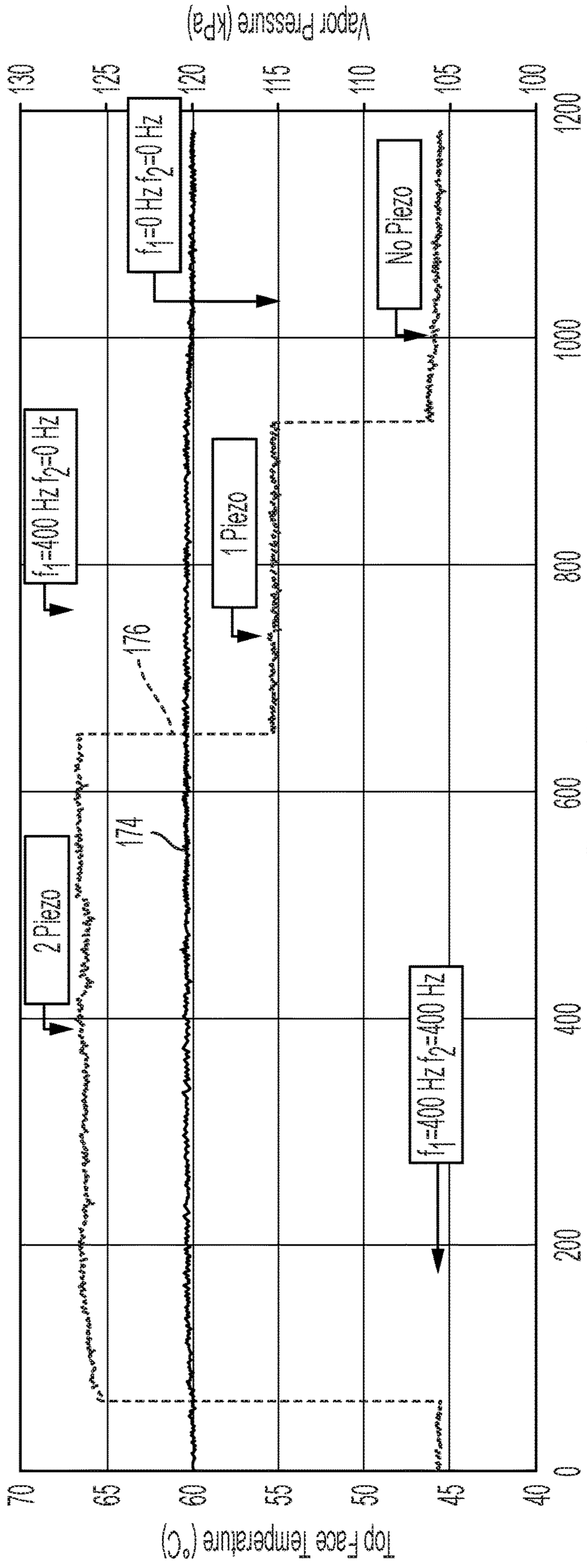
Vapor Pressure (kPa)
130
125
120
115
110
105
100
1200
1000
800
600
400
200
0
Time (seconds)
Top Face Temperature (°C)
70
65
60
55
50
45
40
Top Face Temperature
Vapor Pressure
f1=0 Hz f2=0 Hz
No Piezo
f1=400 Hz f2=0 Hz
1 Piezo
2 Piezo
f1=400 Hz f2=400 Hz
174
176

FIG. 10

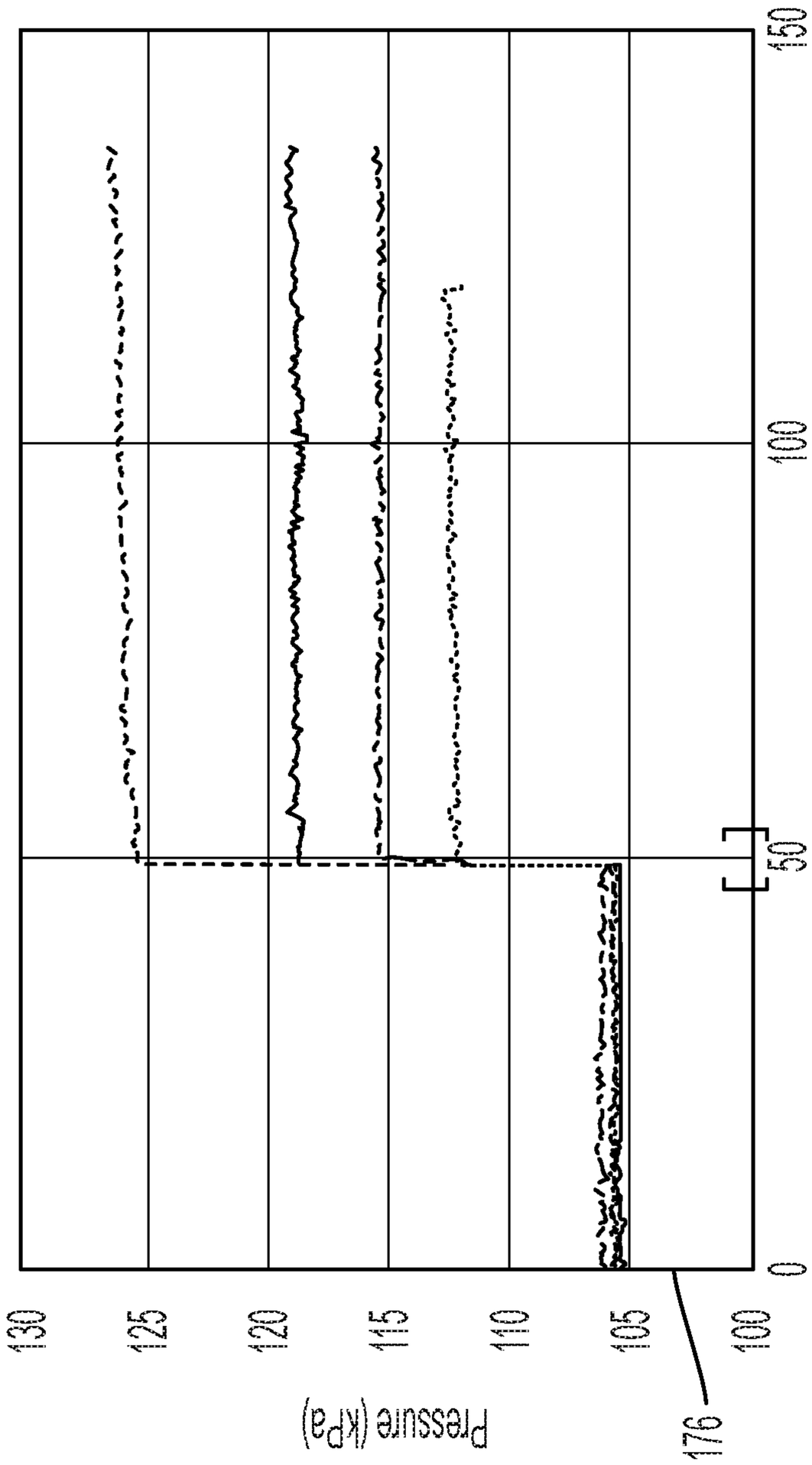
150
100
50
Time (sec)
0.1 s
Piezo f1=f2=420 Hz, 0.5 Duty Cycle
Piezo f1=f2=400 Hz, 0.7 Duty Cycle
Piezo f1=400, f2=0 Hz, 0.7 Duty Cycle
Piezo f1=1200, f2=0 Hz, 0.5 Duty Cycle
130
125
120
115
110
105
100
0
176
Pressure (kPa)

FIG. 11

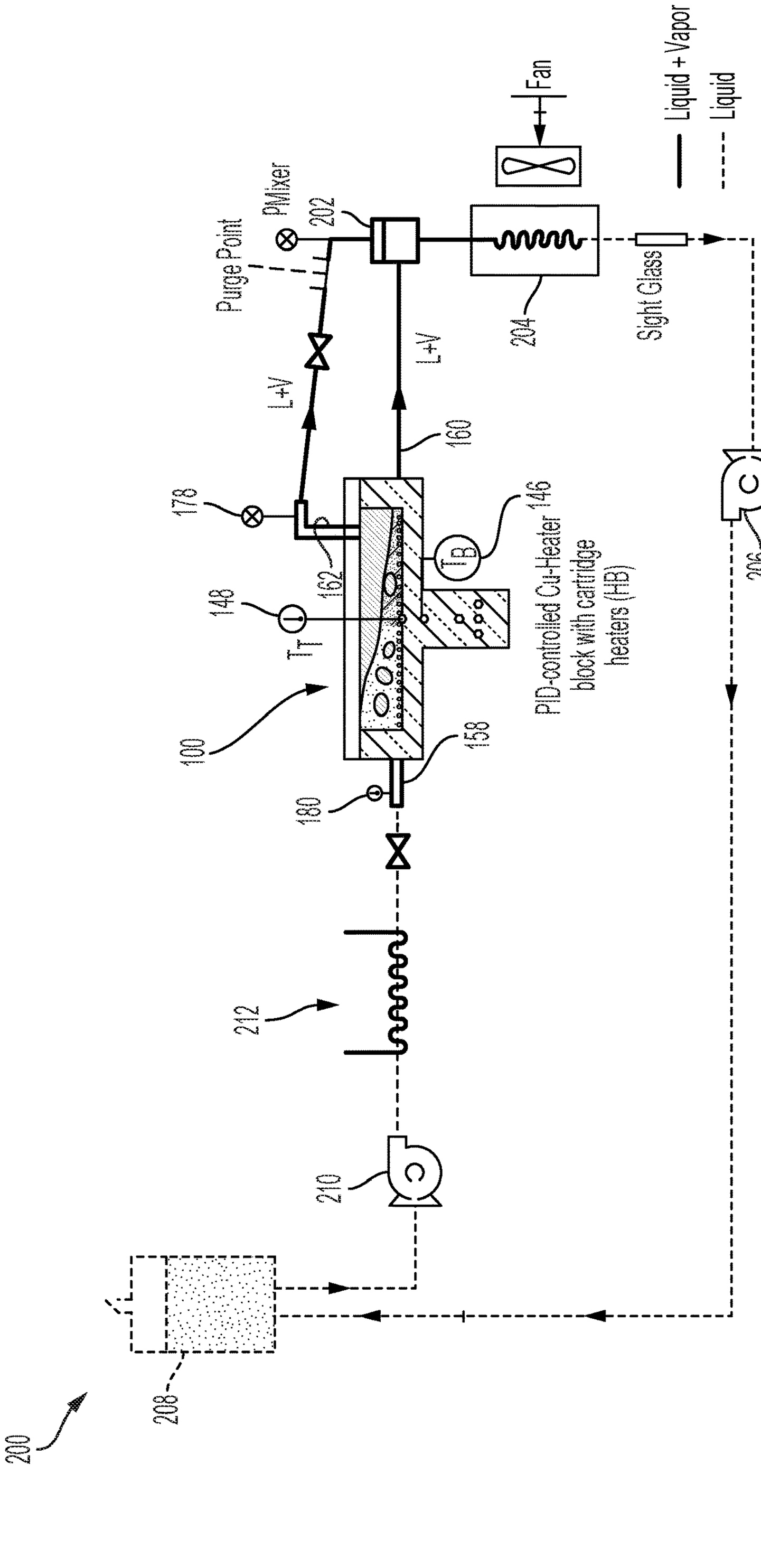
Liquid + Vapor
Liquid
Fan
PMixer
202
Purge Point
L+V
204
Sight Glass
160
178
162
TB
146
148
TT
100
158
180
PID-controlled Cu-Heater block with cartridge heaters (HB)
206
212
210
208
200

FIG. 12

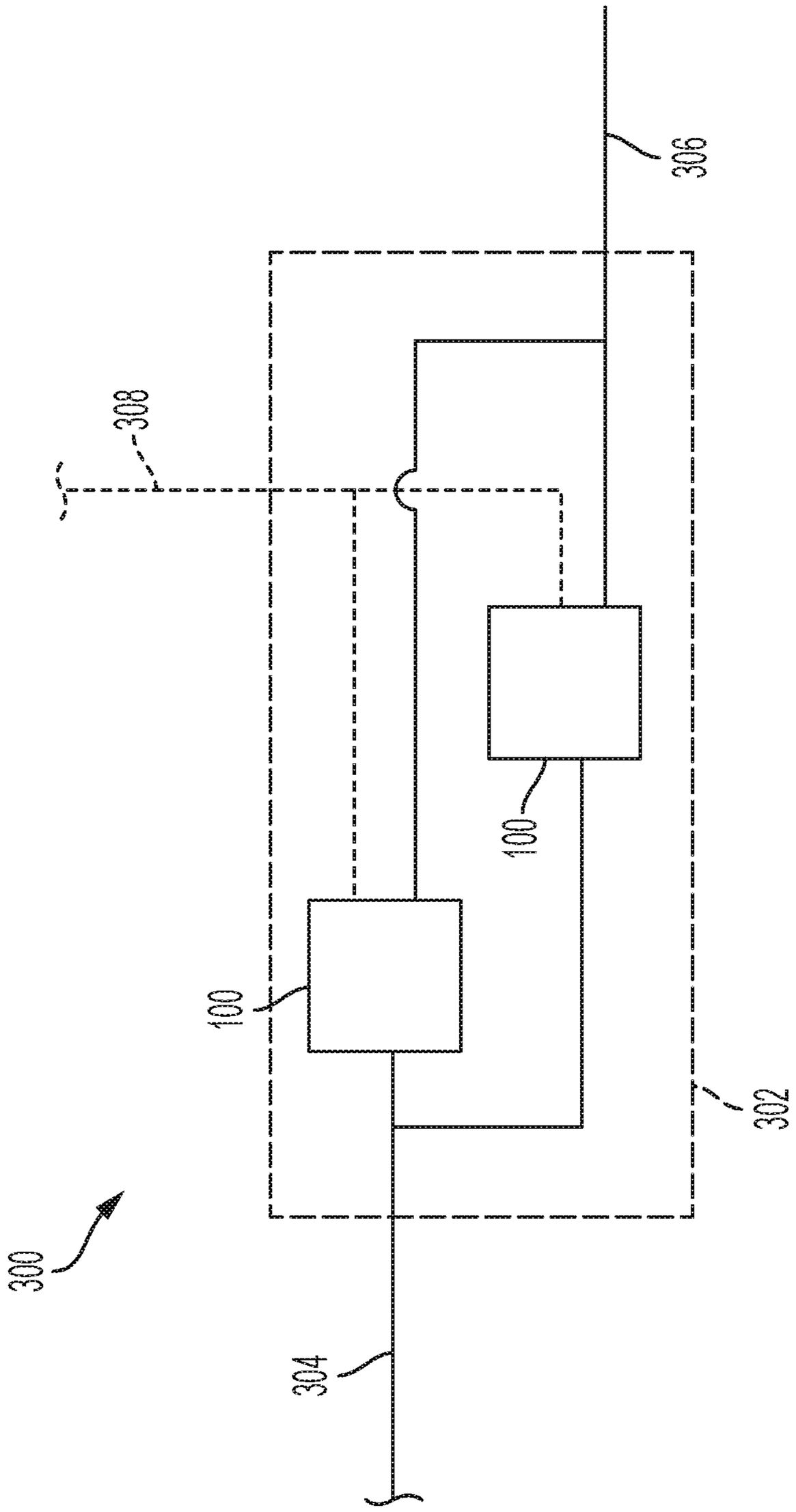

FIG. 13

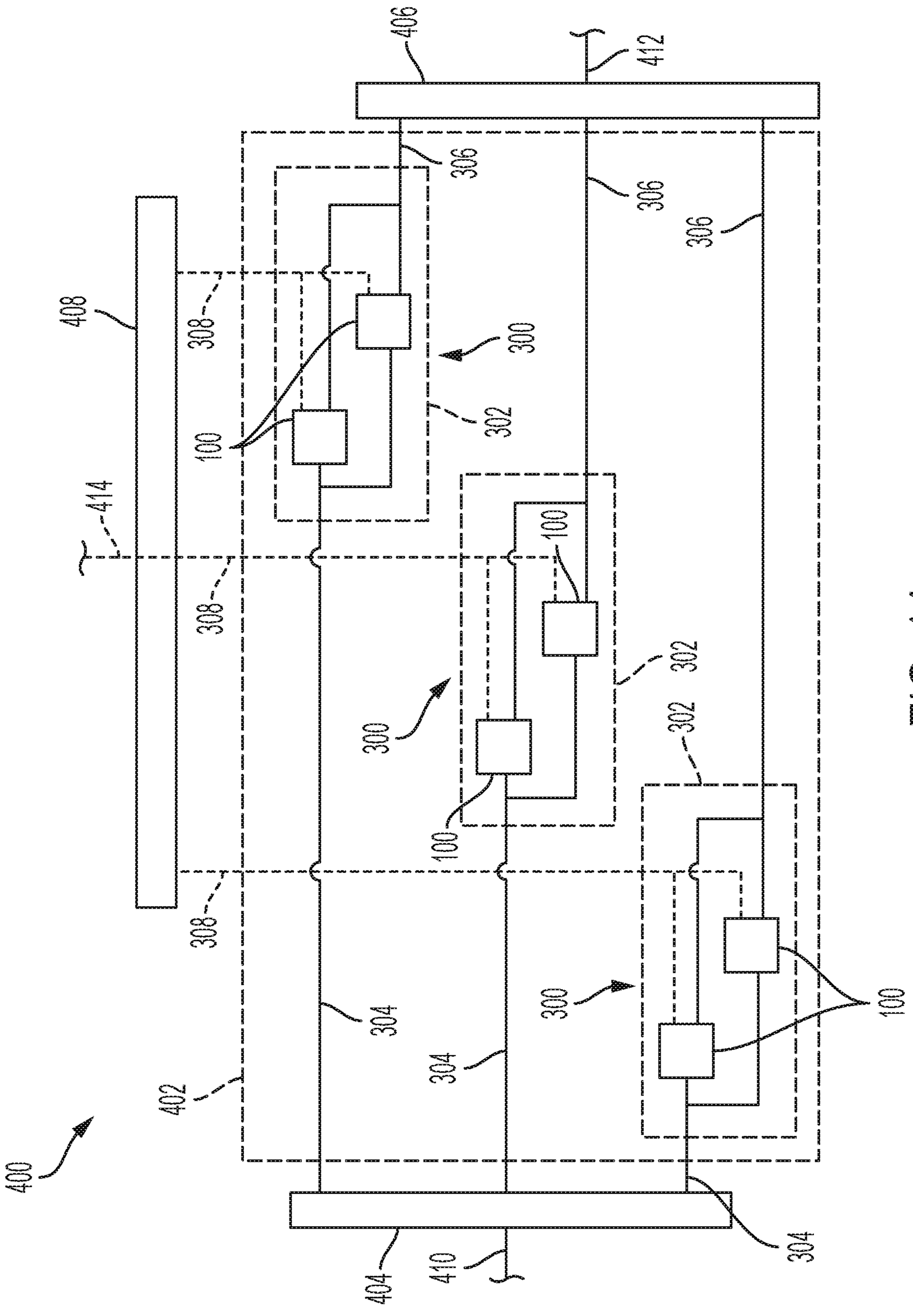
406
412
306
306
306
408
308
308
300
100
302
414
308
100
300
302
302
308
304
304
300
100
402
404
410
304
400

FIG. 14

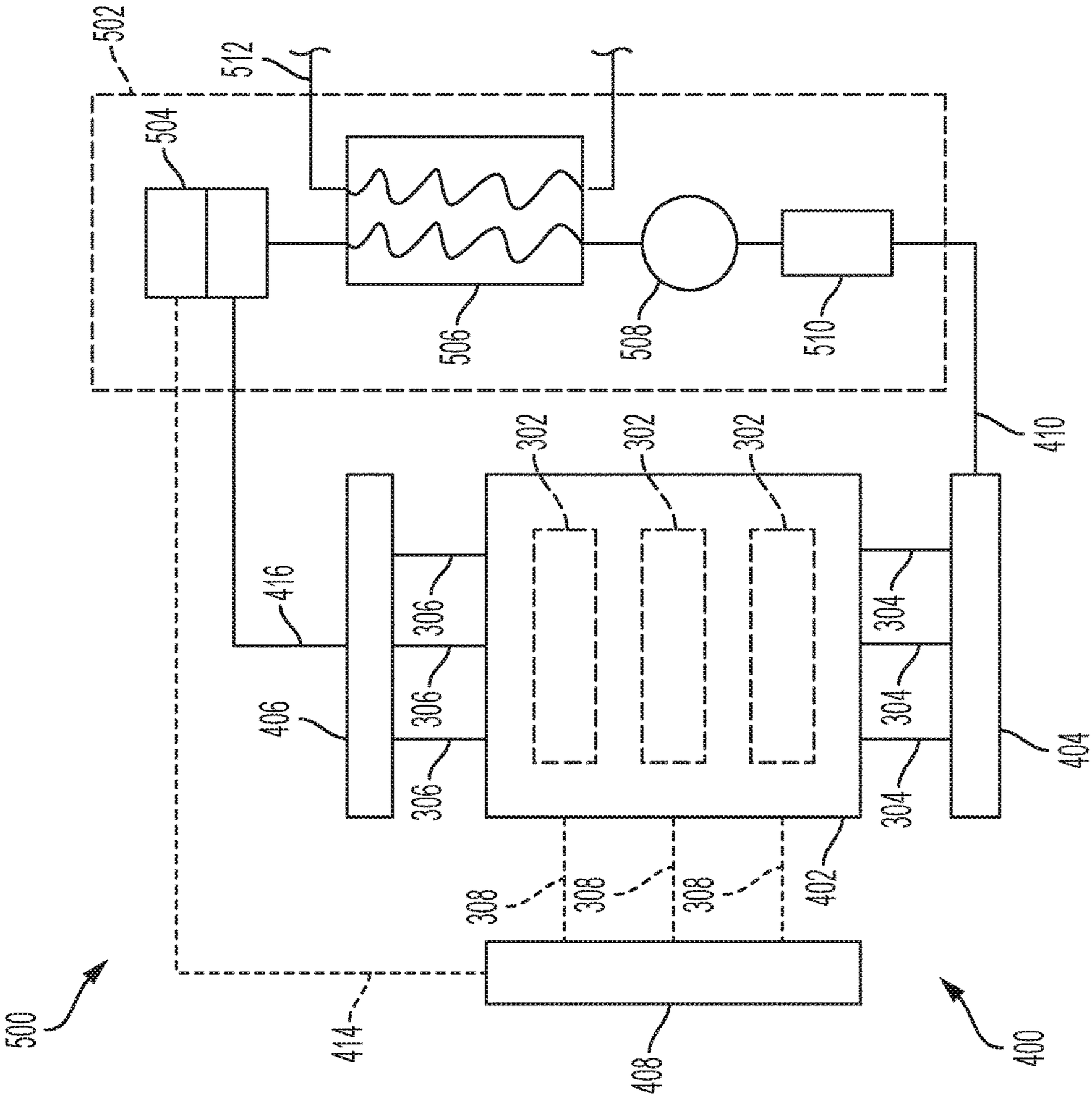
502
512
504
506
508
510
410
302
302
302
416
306
306
306
406
304
304
304
404
308
308
308
402
414
408
500
400

FIG. 15

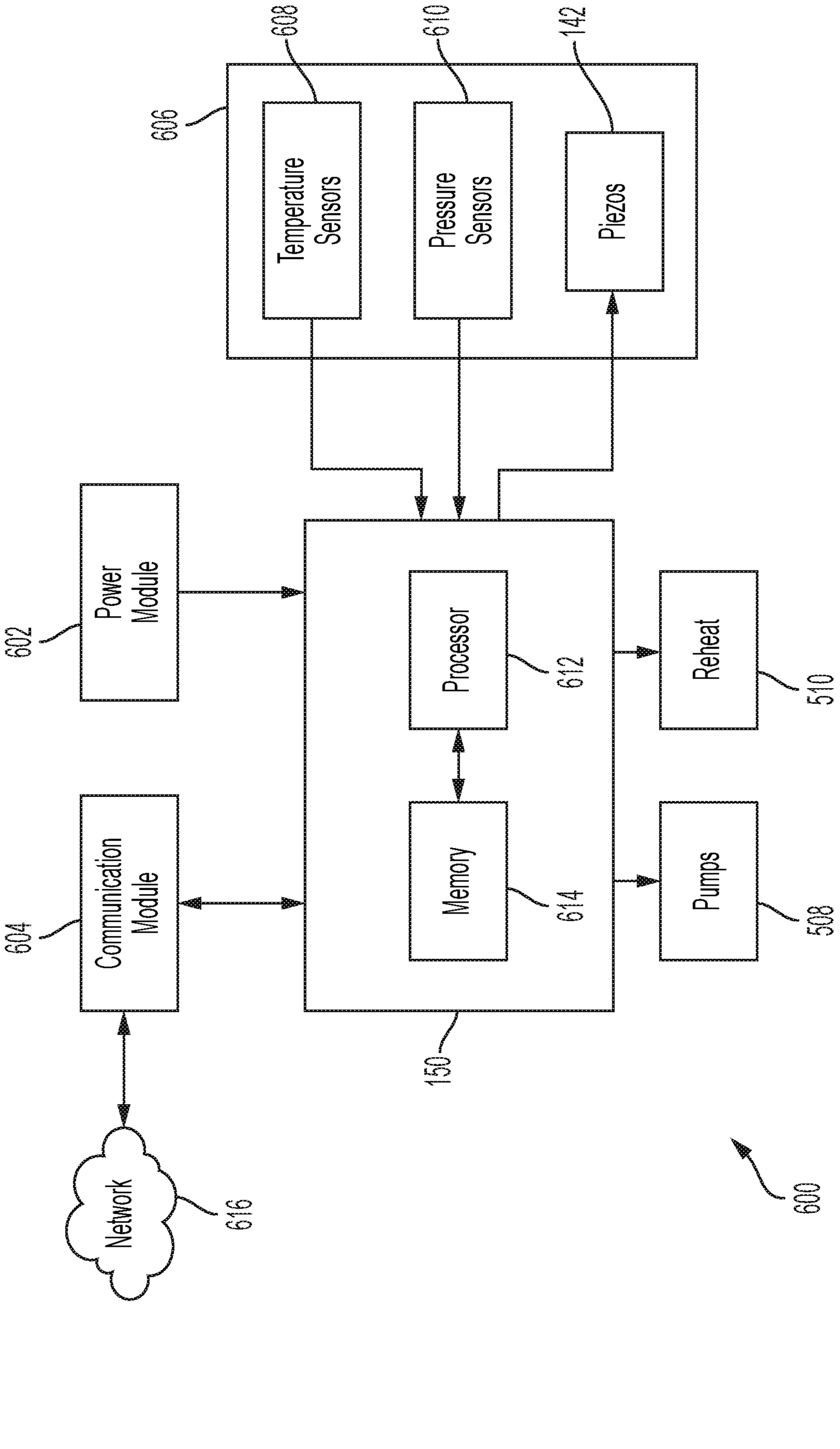
606
608
610
142
Temperature Sensors
Pressure Sensors
Piezos
602
Power Module
604
Communication Module
Network
616
Processor
612
Memory
614
Reheat
510
Pumps
508
150
600

FIG. 16

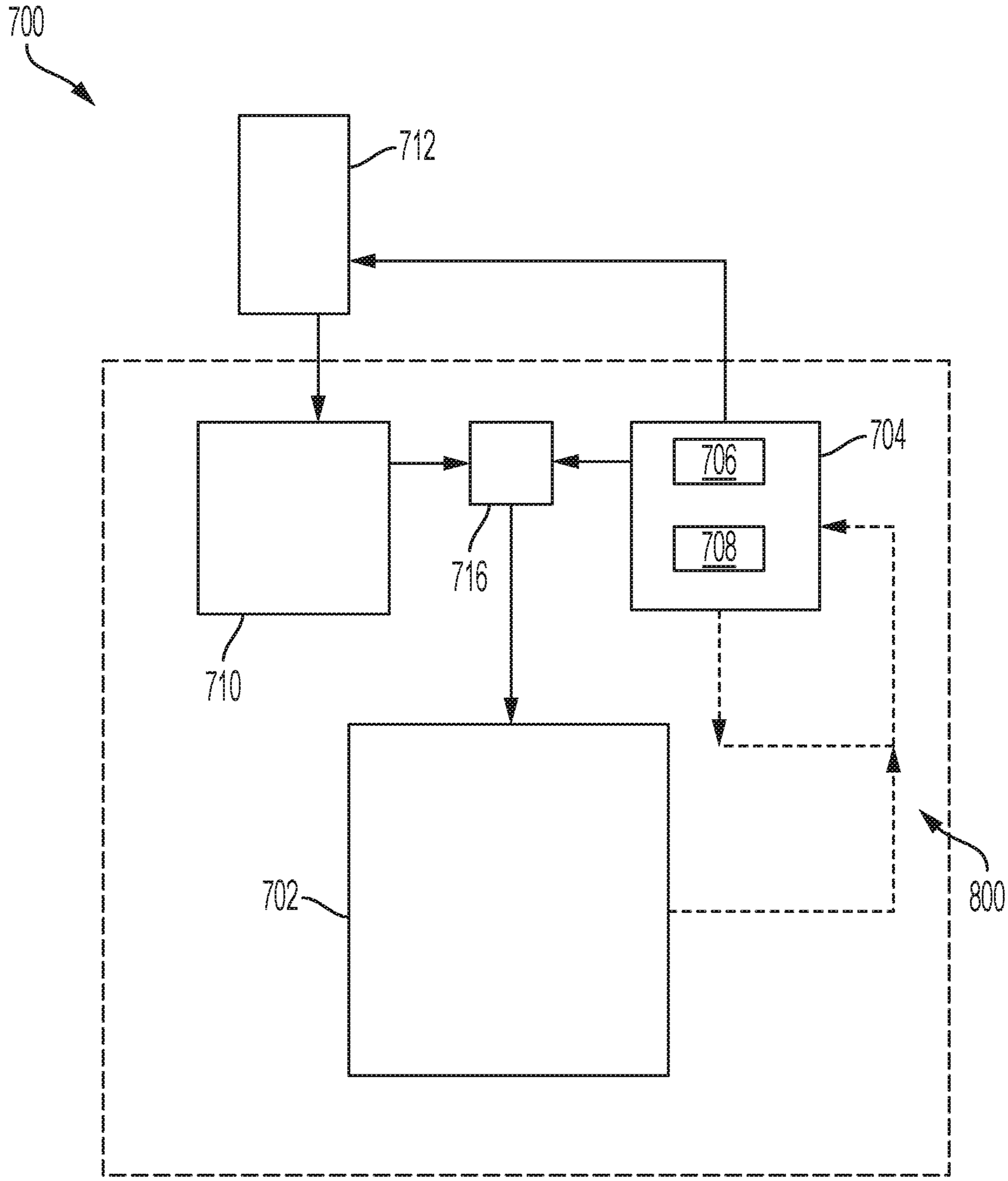

FIG. 17

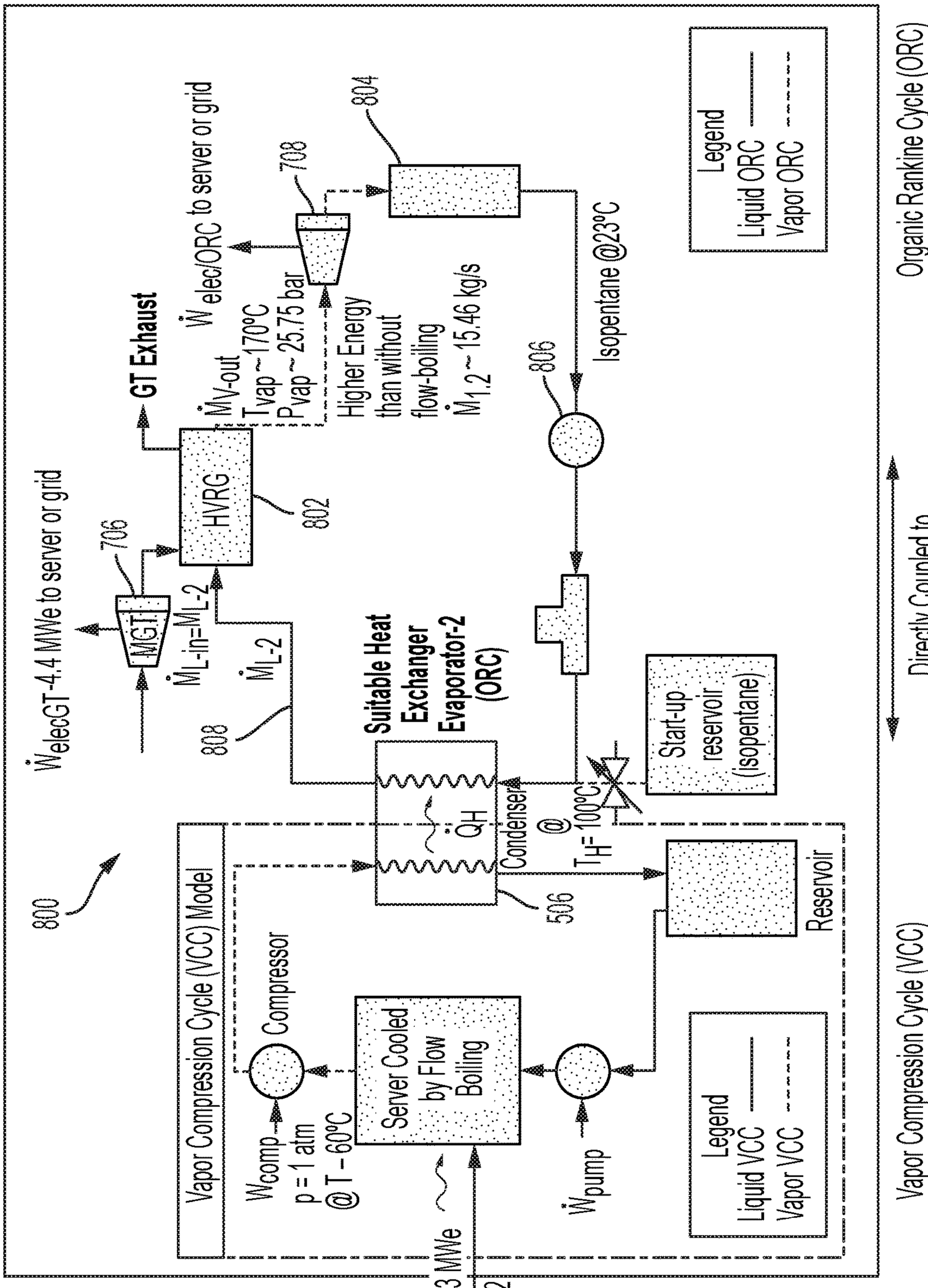
Organic Rankine Cycle (ORC)
Legend
Liquid ORC
Vapor ORC
GT Exhaust
$\dot{W}$ elec/ORC to server or grid
$\dot{M}_{V\text{-}out}$
T_{vap} ~ 170°C
P_{vap} ~ 25.75 bar
Higher Energy than without flow-boiling
$\dot{M}_{1.2}$ ~ 15.46 kg/s
Isopentane @23°C
708
804
806
HVRG
802
706
MGT
$\dot{M}_{L\text{-}in}=\dot{M}_{L\text{-}2}$
$\dot{M}_{L\text{-}2}$
808
$\dot{W}_{elecGT}$-4.4 MWe to server or grid
Suitable Heat Exchanger Evaporator-2 (ORC)
$\dot{Q}_H$
Condenser
506
T_H= 100°C @
Start-up reservoir (isopentane)
Reservoir
800
Directly Coupled to
Vapor Compression Cycle (VCC) Model
Compressor
$\dot{W}_{comp}$
p = 1 atm
@ T – 60°C
Server Cooled by Flow Boiling
$\dot{W}_{pump}$
IT Power = 3.33 MWe
For PUE =1.2
500
Legend
Liquid VCC
Vapor VCC
Vapor Compression Cycle (VCC)

FIG. 18A

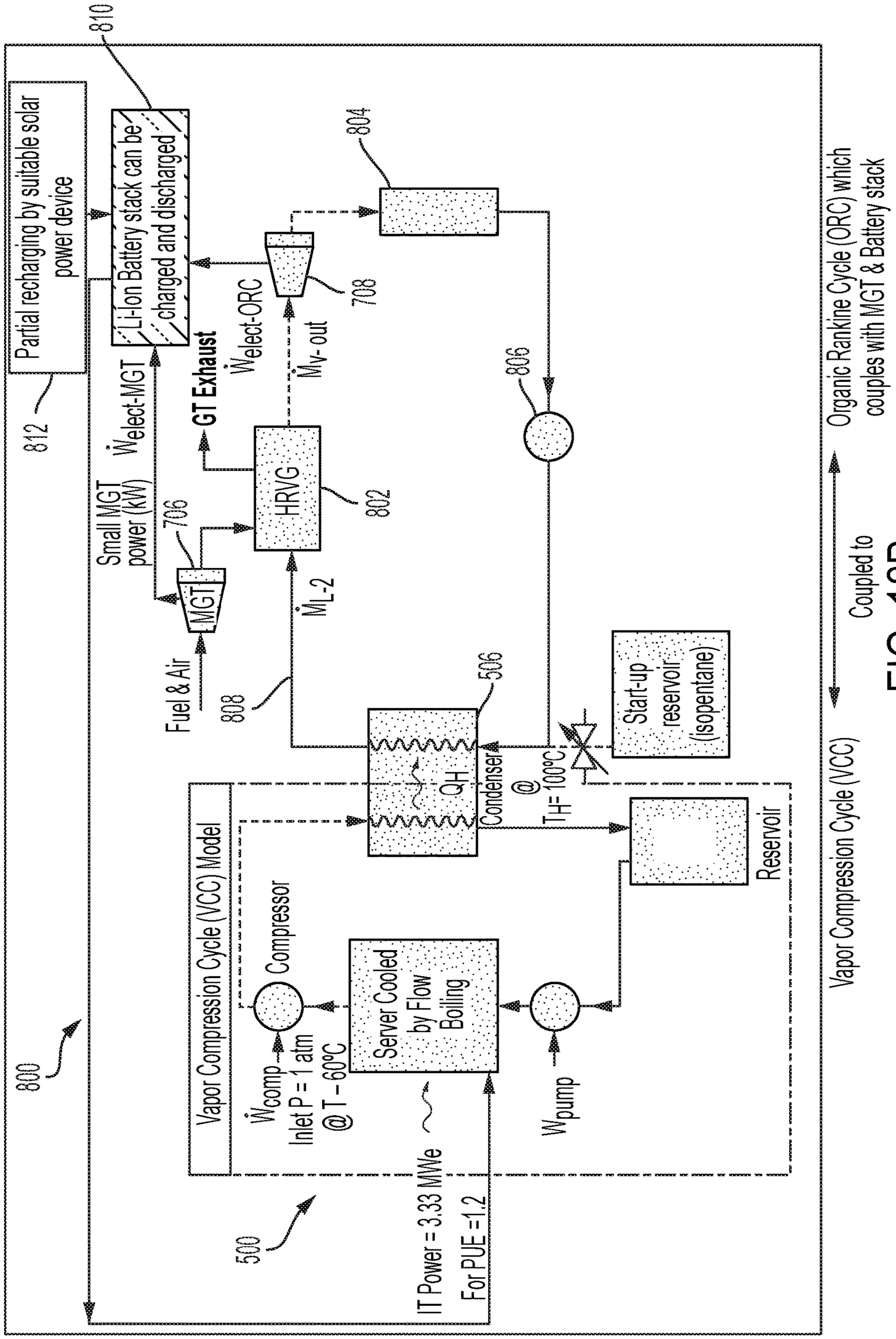
800
Vapor Compression Cycle (VCC) Model
Compressor
Vapor Compression Cycle (VCC)
Coupled to
Organic Rankine Cycle (ORC) which couples with MGT & Battery stack
812
Partial recharging by suitable solar power device
810
Li-ion Battery stack can be charged and discharged
Small MGT power (kW)
Welect-MGT
706
MGT
Fuel & Air
808
GT Exhaust
Welect-ORC
708
Mv- out
804
HRVG
802
ML-2
806
QH
Condenser
506
@ TH= 100°C
Start-up reservoir (isopentane)
Reservoir
Wcomp
Inlet P = 1 atm
@ T – 60°C
Server Cooled by Flow Boiling
Wpump
IT Power = 3.33 MWe
For PUE =1.2
500

FIG. 18B

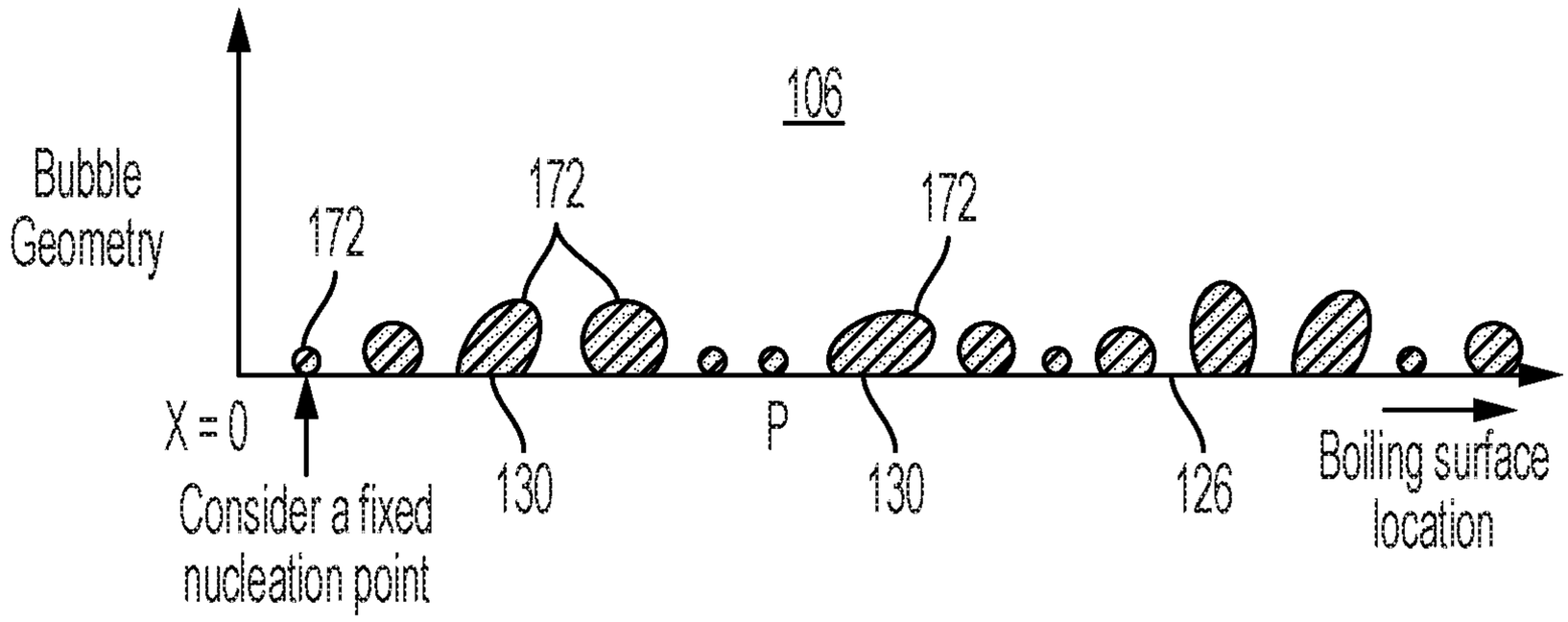

FIG. 19A

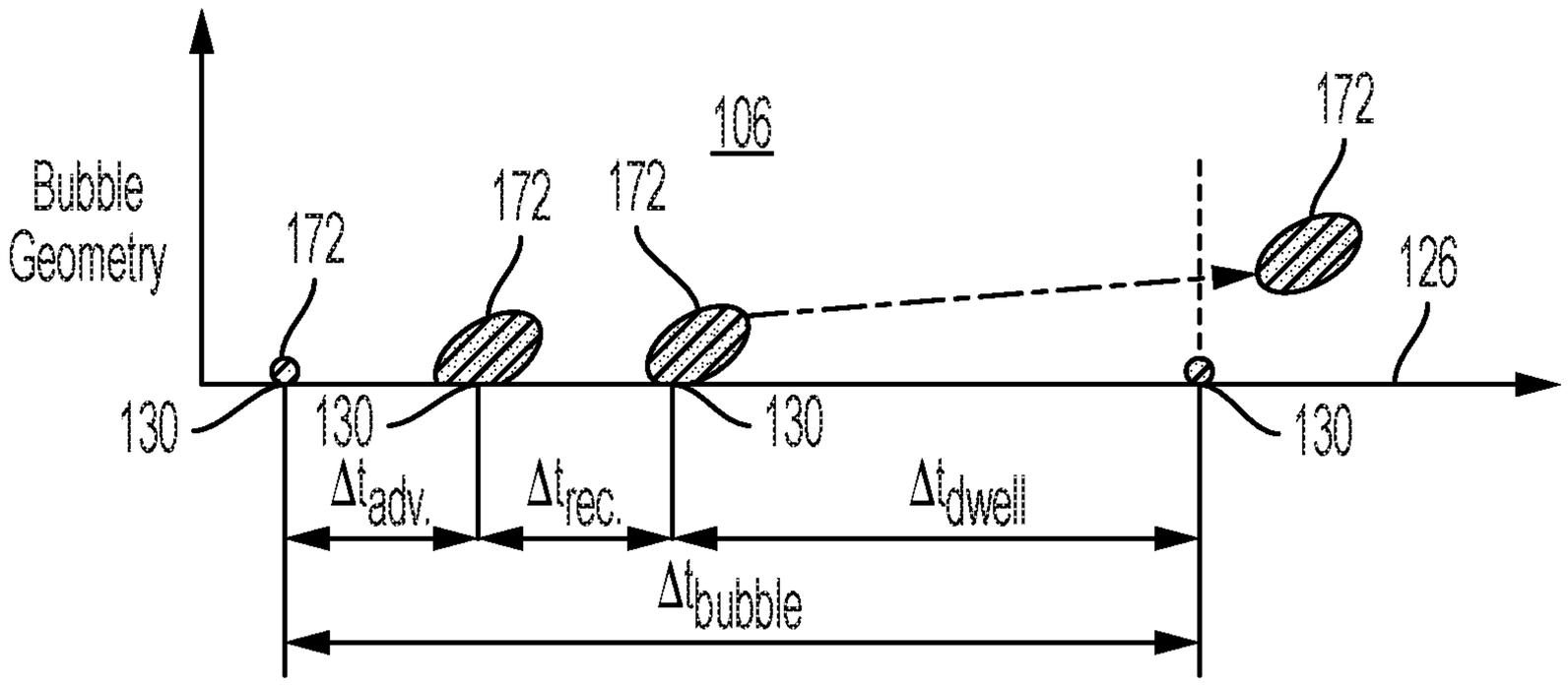

FIG. 19B

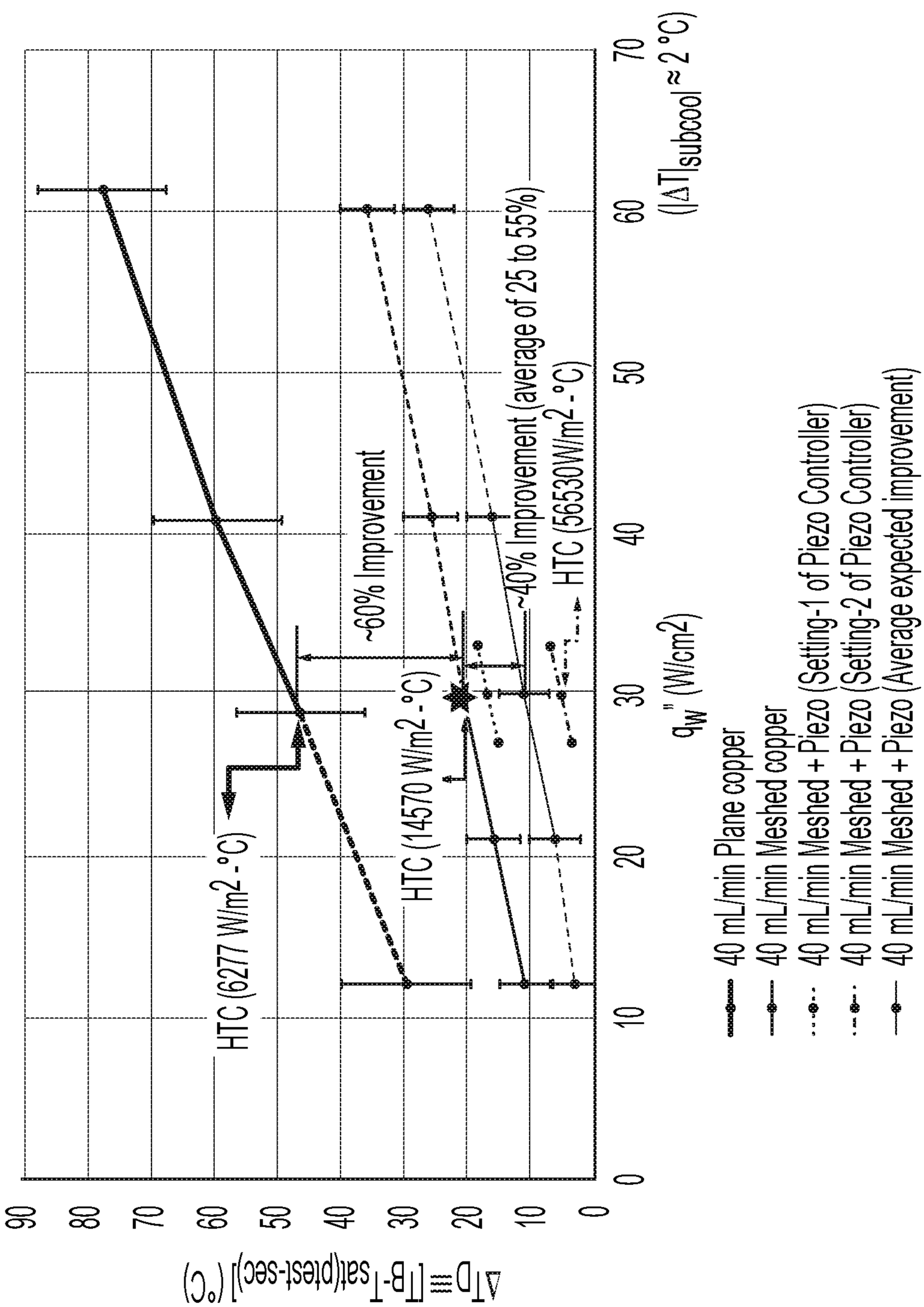
ΔTD≡[TB-Tsat(ptest-sec)] (°C)
0
10
20
30
40
50
60
70
80
90
HTC (6277 W/m2 -°C)
HTC (14570 W/m2 -°C)
~60% Improvement
~40% Improvement (average of 25 to 55%)
HTC (56530W/m2 -°C)
(|ΔT|subcool ≈ 2 °C)
q"W (W/cm2)
0
10
20
30
40
50
60
70
40 mL/min Plane copper
40 mL/min Meshed copper
40 mL/min Meshed + Piezo (Setting-1 of Piezo Controller)
40 mL/min Meshed + Piezo (Setting-2 of Piezo Controller)
40 mL/min Meshed + Piezo (Average expected improvement)

FIG. 20

NUCLEATION CONTROL SYSTEM AND METHOD LEADING TO ENHANCED BOILING BASED ELECTRONIC COOLING

CROSS-REFERENCE TO RELATED APPLICATIONS

This application is a U.S. national stage entry of International Patent Application No. PCT/US2019/060994, filed on Nov. 12, 2019, which claims priority to U.S. Provisional Patent Application No. 62/759,961, filed on Nov. 12, 2018, to U.S. Provisional Patent Application No. 62/833,551, filed on Apr. 12, 2019, and to U.S. Provisional Patent Application No. 62/870,624, filed on Jul. 3, 2019, the contents of all of which are hereby incorporated by reference in their entirety.

BACKGROUND

Flow boiling can be implemented within mini- or micro-channels to transfer heat from a heated surface to a heat transfer fluid. As used herein, the term "microchannel" is intended to refer to a flow channel having a diameter up to about 5-6 millimeters. At the micro scale, and at certain critical heat-flux (CHF) levels, flow instabilities and other duct- and system-level instabilities can induce a dynamic local dry-out phenomenon between the heated surface and attached vapor bubbles. This is more likely at high exit vapor mass qualities.

SUMMARY OF THE INVENTION

The disclosure provides, in one aspect, a cooling module for an electronic device. The cooling module includes a body having formed therein a plurality of channels, a micro-structured boiling surface, a piezoelectric transducer, an inlet header, and an outlet header. Each channel of the plurality of channels is defined by a first channel surface and opposing lateral channel surfaces cooperatively defining a rectangular cross section normal to a channel axis. The micro-structured boiling surface is positioned adjacent the first channel surface of each channel. The piezoelectric transducer is in acoustic communication with one of the opposing lateral channel surfaces of each channel and configured to direct acoustic waves on the micro-structured boiling surface. The inlet header is in fluid communication with each channel of the plurality of channels. The outlet header is in fluid communication with each channel of the plurality of channels.

The disclosure provides, in another aspect, a method of cooling an electronic device. The method includes passing a heat transfer fluid through one or more channels formed in a cooling module body, each channel defined by a first channel surface and lateral channel surfaces and further including a micro-structured boiling surface adjacent the first channel surface. The method also includes energizing a piezoelectric transducer in acoustic communication with one of the opposing lateral channel surfaces of each channel to direct in-plane acoustic waves on the micro-structured boiling surface and its vicinity to facilitate formation of microbubbles within the heat transfer fluid at microbubble nucleation sites on the micro-structured boiling surface.

The disclosure provides, in another aspect, a controller for a server rack cooling loop for cooling a plurality of electronic devices. The controller includes memory and a processor. The processor is configured to receive inputs of a cooling loop temperature and pressure, determine desired flow boiling parameters of the cooling loop, and transmit signals to a piezoelectric transducer in acoustic communication with a flow channel that is in thermal communication with an electronic device. The signals are configured to operate the piezoelectric transducer to resonate a micro-structured boiling surface positioned within the flow channel.

BRIEF DESCRIPTION OF THE DRAWINGS

FIG. **1**A is a perspective view of a cooling unit (e.g., a heat sink) for performing enhanced flow boiling according to one embodiment.

FIG. **1**B is a cross-sectional perspective view of the cooling unit of FIG. **1**A, taken along line **1**B-**1**B of FIG. **1**A.

FIG. **2** is a perspective view of a microchannel of the cooling unit of FIG. **1**A.

FIG. **3** is a cross-sectional schematic illustration of a micro-structured boiling surface of the microchannel of FIG. **2**, taken along line **3**-**3** of FIG. **2**.

FIG. **4** is a perspective view of alternative micro-structured boiling surfaces for use with the microchannel of FIG. **2**.

FIGS. **5**A-**5**E are plan views of alternative mesh structures for forming the micro-structured boiling surface of FIG. **3**.

FIG. **6** is a schematic cross-sectional view of the microchannel of FIG. **2**, taken along line **3**-**3** of FIG. **2**.

FIG. **7** is another schematic cross-sectional view of the microchannel of FIG. **2**, taken along line **7**-**7** of FIG. **2**.

FIG. **8** is a schematic cross-sectional view of the cooling unit of FIG. **1**, taken along line **1**B-**1**B of FIG. **1**A.

FIGS. **9**-**11** are graphs illustrating temperature and pressure information associated with piezos-actuated enhanced flow-boiling operation of the microchannel of FIG. **2**.

FIG. **12** is a schematic illustration of an exemplary cooling loop that incorporates the cooling unit of FIG. **1**A.

FIG. **13** is a schematic illustration of a server-level cooling subsystem for cooling multiple microchips supported on a server board using the cooling unit of FIG. **1**A.

FIG. **14** is a schematic illustration of a rack-level cooling subsystem that incorporates the server-level cooling subsystem of FIG. **13** to cool multiple server boards incorporated into a server rack.

FIG. **15** is a schematic illustration of a server rack cooling loop that incorporates the rack-level cooling subsystem of FIG. **14**.

FIG. **16** is a block diagram of an exemplary control system associated with the server rack cooling loop of FIG. **15**.

FIG. **17** is a schematic illustration of a data center energy system for providing power and thermal management to a data center.

FIG. **18**A is a schematic illustration of a heat recovery system of the data center energy system of FIG. **17**.

FIG. **18**B is a schematic illustration of another embodiment of the heat recovery system of FIG. **18**A.

FIG. **19**A is a schematic illustration of vapor microbubbles forming on and detaching from the micro-structured boiling surface of FIG. **3** at a certain instant.

FIG. **19**B is another schematic illustration of a single vapor microbubble forming on and detaching from the micro-structured boiling surface of FIG. **3**.

FIG. **20** is a graph illustrating reductions in driving temperature-differences for a given heat flux associated with operation of the microchannel of FIG. **2**.

Before any embodiments of the disclosure are explained in detail, it is to be understood that the disclosure is not

limited in its application to the details of the formation and arrangement of components set forth in the following description or illustrated in the accompanying drawings. The disclosure is capable of supporting other embodiments and of being practiced or of being carried out in various ways. Also, it is to be understood that the phraseology and terminology used herein is for the purpose of description and should not be regarded as limiting.

DETAILED DESCRIPTION

FIGS. **1-8** illustrate a "mini" microchannel architecture two-phase cooling unit **100** (e.g., a heatsink **100**) that enhances flow boiling in microchannels. As used throughout, the term "microchannel" is intended to refer to a flow channel having a diameter up to about 5-6 millimeters. With reference to FIGS. **1**A and **1**B, the cooling unit **100** couples to a heat source **102** (e.g., an electronic device such as a microchip, an integrated circuit, etc.) to facilitate removal of heat energy from the heat source **102**. While the illustrated cooling unit **100** is described in connection with cooling electronic devices, other cooling applications are also possible and contemplated herein. As discussed below, the cooling unit **100** significantly enhances flow boiling heat transfer rates as compared to existing flow boiling heat exchangers, as well as commercially available single-phase liquid cooling approaches.

The cooling unit **100** defines a plurality of microchannels **104**. A heat exchanging or cooling fluid **106** (FIG. **2**) is directed to flow through the microchannels **104** to accept and carry away heat energy from the heat source **102**. Although many formulations of cooling fluids are possible, one exemplary, electronics and environment friendly formulation contemplated (and utilized) herein is 3M™ Novec™ Engineered Fluid HFE-7100.

As shown in FIGS. **1** and **8**, the cooling unit **100** includes a base plate **108** that couples to the heat source **102** (e.g., a microchip **164** mounted on a server), and a removable top plate **110** opposite the base plate **108**. The microchannels **104** extend between the bottom and top plates **108**, **110** and generally parallel thereto. Each microchannel **104** is defined between opposing sidewalls **112**, a bottom wall **114** defined by a portion of the base plate **108**, and a top wall **116** defined by a portion of the top plate **110**. In the illustrated embodiment, the sidewalls **112** and the base plate **108** are formed from a thermally-conductive material such as, but not limited to, copper. The top plate **110** may likewise be formed from a thermally-conductive material. In some embodiments, the top wall **116** may be formed from a transparent material (e.g., polycarbonate) that renders the space within the microchannel **104** visible from outside the microchannel **104**. The cooling unit **100** also includes end walls **113** that extend between the bottom and top plates **108**, **110** and laterally contain the microchannels **104**. In some embodiments, thermal sheets (e.g., poly-graphite sheets; not shown) may extend between the base plate **108** and the end walls **113**. The thermal sheets can reduce flow and thermal maldistribution across the microchannels **104**.

With reference to FIG. **2**, the illustrated microchannel **104** has a generally elongated shape extending along a central axis **118** with a generally rectangular cross-section perpendicular thereto, and includes a length **120**, a width **122**, and a height **124**. The length **120** is measured between end portions of the sidewalls **112** in a direction parallel to the central axis **118**. The width **122** is measured between the sidewalls **112** in a direction perpendicular to the sidewalls **112** and generally transverse to the central axis **118**. The height **124** is measured between the bottom and top walls **114**, **116**. For the illustrated microchannel **104** of FIG. **2**, the length **120** is approximately 50 millimeters (mm), the width **122** is approximately 10 mm, and the height **124** is approximately 5 mm. Accordingly, the illustrated microchannel **104** includes a "mini-channel" construction (i.e., as compared to many existing micron-scale channels having channel width/height dimensions on the order of 600 micrometers (μm) or less). Such a "mini-channel" construction is sought because of a need to meet average heat-flux impositions from the heat source **102** in the range of 50-100 W/cm^2 or higher, as large values of total mass-flux (G) and very large vapor volume fluxes are required for such high heat-flux values, which lead to large pumping powers and unacceptable performances (flow instabilities, etc.).

With reference to FIG. **8**, the bottom wall **114** defines and/or at least partially supports a micro-structured boiling surface **126** that faces an interior of the microchannel **104**. During operation of the cooling unit **100**, the cooling fluid **106** undergoes a flow boiling process within each microchannel **104**. A major component the flow boiling process involves nucleation, growth, and detachment of micron-scale (μm) vapor microbubbles transpiring at the micro-structured boiling surface **126**. Stimulating the formation and subsequent detachment of these vapor microbubbles leads to a significant enhancement in the heat transfer coefficient (HTC) of the flow boiling process.

To enhance the rates of vapor bubble nucleation, growth, and detachment, the micro-structured boiling surface **126** is defined by a plurality of interconnected micro-structures **128** (FIG. **3**) that extend upward from the bottom wall **114** into the microchannel **104**. The micro-structures **128** of the micro-structured boiling surface **126** (FIG. **2**) define numerous vapor bubble nucleation sites **130** (FIG. **3**) distributed evenly across the boiling surface **126**. By providing the micro-structured boiling surface **126** on the bottom wall **114**, a number density per unit area of the vapor bubble nucleation sites **130** is dramatically increased for wetting fluids **106** as compared to that of many existing flow boiling heat exchangers employing a generally smooth boiling surface devoid of micro-structures. In other embodiments, the micro-structured boiling surface **128** can be chemically (or equivalent) formed, leading to a judicious mix of wetting and non-wetting microstructured surfaces.

As schematically illustrated in cross-section in FIG. **3**, the interconnected micro-structures **128** include a base **132** attached to the bottom wall **114**, and a distal end **134** opposite the base **132**. A micro-structure height **136** is measured between the base **132** and the distal end **134**, and a micro-structure spacing **138** measured between adjacent micro-structures **128**. The illustrated micro-structured boiling surface **126** includes a micro-structure height **136** of approximately 450 and a micro-structure spacing **138** of approximately 150 μm.

In the illustrated embodiment, the interconnected micro-structures **128** of the illustrated microchannel **104** are formed by affixing a micro-structured mesh **140** (FIG. **5**A) to the bottom wall **114** to create the micro-structured boiling surface **126**. In some embodiments, this can be performed by diffusion bonding one or more layers of the micro-structured mesh **140** (e.g., four layers) to the bottom wall **114**. The illustrated mesh **140** is formed from the same material as the bottom wall **114** (e.g., a material having high thermal conductivity, such as copper), although other mesh materials are also possible. In some embodiments (not shown), the distal end **134** (FIG. **3**) may be made of a porous layer of the metal used.

FIG. **4** illustrates additional, non-limiting examples of micro-structured boiling surfaces **126***a*-**126***f*. While several variations in height, spacing, and pattern are possible, each of the illustrated interconnected micro-structures defining the boiling surfaces **126***a*-**126***f* increase the vapor bubble nucleation site density. FIGS. **5**B-**5**E illustrate additional, non-limiting examples of various micro-structured meshes **140***a*-**140***d* which may be utilized to form the micro-structured boiling surface **126**.

With reference to FIG. **6**, the illustrated cooling unit **100** also includes piezoelectric-transducers **142** (hereinafter, "piezos **142**") mechanically and acoustically coupled to each sidewall **112**. In the illustrated embodiment, the piezos **142** are located external to the microchannels **104**. Each piezo **142** includes an output face **143** facing toward an interior of each respective microchannel **104**. The piezos **142** are arranged transverse to the micro-structured boiling surface **126**, so as to direct acoustic waves incident on the micro-structured boiling surface **126** (i.e., so as to propagate within a plane defined by the boiling surface **126**), as well as incident on its upper and lower vicinities. The upper vicinity includes the cooling fluid **106** flowing through the microchannel **104**. As shown in FIG. **8**, in the illustrated embodiment, a pair of piezos **142** are associated with each microchannel **104**, with the output faces **143** of each piezo **142** of the associated pair facing inward toward the interior of the microchannel **104**, and facing toward each other. In other embodiments (not shown), just a single piezo **142** can be associated with each respective microchannel **104**. In further embodiments, more than two piezos **142** can be associated with each microchannel **104**. An acoustic gel **144** is disposed between each piezo **142** and each associated sidewall **112** to facilitate the transmission of acoustic waves into the microchannel **104**. In some embodiments, each sidewall **112** can have a thickness T (FIG. **8**) close to a quarter wave-length for that material. As shown in FIG. **2**, each piezo **142** extends along a direction of the height **124**, so as to overlap the base plate **108**, the micro-structured boiling surface **126** (as shown in FIG. **6**), and a portion of the interior of the microchannel **104** through which the cooling fluid **106** flows. Each piezo **142** likewise extends along a direction of the length **120** (FIG. **2**) and overlaps much of the length **120** of each microchannel **104**.

In the illustrated embodiment, the piezos **142** are transverse mode piezoelectric transducers **142** (e.g., PZT-5A type) having a resonant frequency $f_p=(\Delta t_{piezo})^{-1}$. In the present embodiment, the resonant frequency f_p is about 1 megahertz (MHz), although other types of piezoelectric transducers having resonant frequencies other than 1 MHz are also contemplated. The transverse mode piezos **142** are arranged and oriented, as described above, to introduce longitudinal acoustic waves in the base plate **108**, in the micro-structured boiling surface **126**, and within the adjacent cooling fluid **106**. The acoustic waves (typically in the 1-2000 Hz range) are introduced by interference of waves obtained by modulating, at acoustic wave frequencies, the natural resonant frequency f_p (about 1 MHz) transverse waves from the piezos **142**. These tunable modulations are obtained by an "on-off" frequency superposition (or equivalent) available with the controller driving the piezos **142**. This approach of arriving at acoustic range modulation frequencies are also effective in significantly reducing noise-levels associated with such signals (this is because most of the energies are at inaudible frequency ranges).

The piezos **142** are operable to introduce acoustic waves A_{wire}, A_{cu}, and A_{fluid} (FIG. **6**) at modulation frequencies appropriate for inducing resonance with the "in-plane" natural frequencies of the micro-structured boiling surface **126**, frequencies associated with aggregate microbubble ebullition cycles on the boiling surface **126**, and suitable hydrodynamic acoustic force frequencies that act on the microbubbles when formed within the cooling fluid **106**, respectively. The acoustic waves A_{wire}, A_{cu}, and A_{fluid} are "in-plane" acoustic waves, meaning they are dominant in planes defined by the micro-structured boiling surface **126** as well as in planes parallel thereto. In the embodiment shown in FIG. **6**, the in-plane acoustic waves propagate back and forth between the opposed sidewalls **112** and are dominant in directions indicated in FIG. **6** as A_{wire}, A_{cu}, and A_{fluid} and in FIG. **3** as A_{wire}. As will be further discussed below, differences in the amplitude and energy of the acoustic waves A_{wire}, A_{cu}, and A_{fluid} result in the introduction of oscillatory in-plane shear stresses S_x and S_y (FIGS. **6** and **7**) at the micro-structured boiling surface **126**.

With reference to FIGS. **6** and **7**, the cooling unit **100** includes one or more temperature sensors disposed within or without one or more of the microchannels **104** for detecting operating temperatures of the cooling unit **100** at one or more locations. In the illustrated embodiment, a first temperature sensor **146** is positioned at a bottom face of the base plate **108**, where the base plate **108** interfaces with the heat source **102**. A second temperature sensor **148** is positioned within the microchannel **104** (e.g., at the micro-structured boiling surface **126**). The temperature sensors **146**, **148** communicate temperature information to a controller **150** (FIG. **16**) associated with the cooling unit **100** (FIGS. **1** and **8**), as will be discussed in further detail below.

With reference to FIGS. **1**A and **1**B, in addition to the microchannels **104**, the cooling unit **100** also includes an inlet header section **152** and an outlet header section **154** disposed at opposite ends of the cooling unit **100**. Each header section **152**, **154** forms a compartment or cooling fluid collection area **156**, and the inlet header section **152** fluidly communicates with the outlet header section **154** via the microchannels **104**. The inlet header section **152** includes an inlet port **158** by which the cooling fluid **106** enters the inlet header section **152**, and the outlet header section **154** includes a primary outlet port **160** (FIG. **12**) by which some or all of the cooling fluid **106** exits the outlet header section **154**. An inlet temperature sensor **180** is located at or near the inlet port **158** to detect a temperature of the cooling fluid **106** entering the cooling unit **100**.

With reference to FIG. **7**, in addition to the primary outlet port **160** (for mostly liquid flows), the outlet header section **154** also includes a secondary outlet port **162** (for mostly vapor flows) that provides a second exit for the cooling fluid **106** to leave the cooling unit **100**. The secondary outlet port **162** is located closer to the top plate **110** (FIG. **1**A) than is the primary outlet port **160**. In some embodiments, the secondary outlet port **162** is provided in the top plate **110**. As will be discussed further below, during operation of the cooling unit **100**, at least some of the cooling fluid **106** flowing through the cooling unit **100** undergoes a phase change from liquid to vapor, due to the enhanced flow boiling occurring within the microchannels **104**. The cooling fluid **106** that remains mostly in the liquid state exits the cooling unit **100** via the primary outlet port **160**, and the cooling fluid **106** that changes to a vapor state exits the cooling unit **100** primarily via the secondary outlet port **162**. The secondary outlet port **162** helps to suppress system-level instabilities that otherwise may result from having only a primary outlet port **160**. An absolute pressure transducer **178** is positioned within the secondary outlet port **162** to detect the pressure within the cooling unit **100**.

FIG. **8** is a cross sectional view illustrating the cooling unit **100** mounted on a microchip **164**. The microchip **164** is coupled to a substrate **166** (e.g., a circuit board such as a server board). In some embodiments, a thermally conductive material (TIM) **168** is disposed between a top surface of the microchip **164** and a bottom surface of the base plate **108** to reduce a thermal resistance of the assembly. During operation, the microchip **164** generates waste heat (e.g., at an average heat flux of 6 W/cm^2, roughly equivalent to that of an Intel Xeon® processor) that is conducted through the TIM **168** (if present), the base plate **108**, and toward the micro-structured boiling surface **126**.

FIG. **8** also illustrates interstitial spaces **170** defined between the sidewalls **112** of adjacent microchannels **104**. In the illustrated embodiment, two piezos **142** are located within each interstitial space **170** between two adjacent microchannels **104**, with the two piezos **142** facing opposite directions so as to direct acoustic waves toward an interior of each respective microchannel **104** of the two adjacent microchannels **104**.

In operation, heat generated by the heat source **102** (e.g., the microchip **164**; FIG. **8**) is conducted toward the micro-structured boiling surface **126**. The piezos **142** are energized to introduce acoustic waves A_{cu} and A_{wire} to resonate the base plate **108** and the micro-structured boiling surface **126**, respectively. When energized, the piezos **142** also introduce acoustic waves A_{fluid} to excite the cooling fluid **106**. The cooling fluid **106**, having an inlet quality of zero (i.e., all liquid phase), enters the cooling unit **100** through the inlet port **158** at a temperature just below the saturation temperature (e.g., 2-3° C. subcooled). Subcooled cooling fluid **106** is supplied below the saturation temperature to ensure proper flow-loop operations and purely liquid phase cooling fluid **106** entering the cooling unit **100**. The cooling fluid **106** is not significantly sub-cooled, which could potentially impair the cooling efficiency of the cooling unit **100**. The liquid phase cooling fluid **106** passes through the collection area **156** of the inlet header section **152** and flows into the microchannels **104** (FIG. **1**B). As the liquid phase cooling fluid **106** flows through each microchannel **104**, the cooling fluid **106** interacts with the micro-structured boiling surface **126** such that microbubbles **172** (FIG. **6**) begin to form at the microbubble nucleation sites **130** (FIG. **3**) distributed on the micro-structured boiling surface **126**. As the microbubbles **172** nucleate, grow, and detach from the nucleation sites **130**, heat energy is carried away from the micro-structured boiling surface **126** due to the enthalpy associated with the phase change of the cooling fluid **106** from liquid to vapor phase.

FIGS. **19**A and **19**B respectively illustrate spatial and temporal schematics of micron-scale microbubbles **172** (e.g., having diameters of 10 μm or less) forming on the micro-structured boiling surface **126** and detaching therefrom during the flow boiling process occurring within the microchannels **104**. With reference to FIG. **19**A, at any instant time t, micron-scale microbubbles **172** are forming or otherwise residing, at various stages of development, at the nucleation sites **130** of the micro-structured boiling surface **126**. With reference to FIG. **19**B, for a single fixed nucleation site **130**, a time evolution of a single microbubble **172** is described. The microbubble **172** forms at t=0. The microbubble **172** enlarges in volume during a growth stage Δtadv, and then the microbubble **172** begins to separate from the nucleation site **130** during a detachment stage Δt_{rec}. At the end of the detachment stage Δt_{rec}, the microbubble **172** detaches from the nucleation site **130**. The nucleation site **130** then undergoes a period of dormancy Δt_{dwell} during which there is no microbubble forming at the nucleation site **130**. At the end of the dormancy period Δt_{dwell}, a new microbubble begins to form at the nucleation site **130** and the process is repeated. Resonance is induced for the micro-structures **128** on the base plate **108** by the acoustic waves A_{cu} and A_{wire} (generated by the piezos **142**) incident on the micro-structured boiling surface **126**. As discussed above, the acoustic waves A_{cu} and A_{wire} mechanically stimulate or actuate the detachment of the microbubbles **172** from the nucleation sites **130**. In turn, this reduces the duration of the overall time evolution of the microbubble **172**, resulting in faster flow boiling and improved heat transfer from the micro-structured boiling surface **126** to the cooling fluid **106**.

As discussed above with respect to FIGS. **2** and **3**, the interconnected micro-structures **128** defining the micro-structured boiling surface **126** contribute to a far greater density of microbubble nucleation sites **130** distributed about the micro-structured boiling surface **126**, as compared to boiling surfaces of traditional flow boiling heat exchangers. The relatively greater nucleation site density enhances the rate of microbubble formation and detachment during operation of the cooling unit **100**. As a result, a cooling capacity of the cooling unit **100** is increased—while retaining the liquid wettability—as compared to traditional flow boiling heat exchangers lacking micro-structured boiling surfaces.

Differences in the amplitude and energy of the acoustic waves A_{cu}, A_{fluid}, and A_{wire} (FIGS. **6**-**7**) further aid in the introduction of oscillatory in-plane shear stresses S_x and S_y at the micro-structured boiling surface **126**. The oscillatory shear stresses S_x and S_y (along with a suitable but limited extent of distal tip **134** (FIG. **3**) undergoing in plane vibrations) facilitate in providing resonance opportunities associated with the bubble ebullition cycle frequencies (FIG. **17**B) towards the dislodging of the micron-sized microbubbles **172** from the nucleation sites **130** to enhance flow boiling. The frequency and energy content of the waves A_{cu}, A_{fluid}, and A_{wire} are tuned, by exploration, to the typically unknown aggregate natural frequencies (or a range of frequencies) associated with various nucleation processes of the microbubbles **172**, and with the mesh micro-structures **128** defining the micro-structured boiling surface **126**. In addition, the standing waves within the liquid phase cooling fluid **106** near the saturation temperature can provide additional hydrodynamics forces for dislodging the microbubbles **172**. Introducing oscillatory shear stresses S_x and S_y using transverse mode piezos **142** arranged and oriented as described above was assessed to be superior as compared to use of commercially available shear mode piezos.

The microbubbles **172** forming and detaching during the flow boiling process introduce vapor phase cooling fluid **106** into the microchannels **104**. As the cooling fluid **106** passes through the microchannels **104** and undergoes flow boiling, the amount of vapor phase cooling fluid **106** increases while the amount of liquid phase cooling fluid **106** simultaneously decreases. Accordingly, the cooling fluid **106** has a non-zero outlet quality (i.e., at least some vapor phase cooling fluid **106** is present) upon reaching the fluid collection area **156** of the outlet header section **154**. In some embodiments, the outlet quality of the cooling fluid **106** can be in the range of 0.05-1.00. In other embodiments, the flow rates are matched to heat loads and the outlet quality is kept in the range of 0.4-0.6 in order to avoid certain dry-out related and other types of flow instabilities.

After reaching the fluid collection area **156** of the outlet header section **154**, the cooling fluid **106** then exits the cooling unit **100** via one or both of the primary and secondary outlet ports **160**, **162**. In the illustrated embodiment, a mixture of vapor and liquid phase cooling fluid **106** exits the cooling unit **100** through the primary outlet port **160**, while predominantly vapor phase cooling fluid **106** exits through the secondary outlet port **162**.

FIGS. **9-11** and **20** depict graphs showing temperature and pressure data collected while operating the microchannel **104** shown in FIG. **2**. A top face temperature **174** was measured by the second temperature sensor **148** positioned at the micro-structured boiling surface **126**, and a vapor pressure **176** was measured by the absolute pressure transducer **178** located within the secondary outlet port **162**.

With reference to FIG. **9**, in one test, the microchannel **104** was initially operated with the piezos **142** switched off from time=0 seconds until time=40 seconds. During this initial time period, the top face temperature **174** remained relatively constant at about 60° C., and the vapor pressure **176** likewise held stable at about 106 kPa. At time=40 s, both of the two piezos **142** associated with the microchannel **104** were switched on. A rapid increase in the vapor pressure **176** was detected within the microchannel **104** in response to activation of the piezos **142**, increasing from about 106 kPa to about 120 kPa. However, the top face temperature **174** continued to measure near 60° C. after the piezos **142** were switched on. At time=180 s, both piezos **142** were switched off, and the vapor pressure **176** rapidly fell back toward 106 kPa. The rapid increase in vapor pressure **176** in response to activation of the piezos **142** is attributable to an increase in the rate of microbubble nucleation, growth, and detachment while the liquid flow rate (FIG. **12**) downstream of the condenser and upstream of the inlet **158** stayed constant. The microbubble nucleation rates are stimulated by the acoustic waves A_{cu}, A_{fluid}, and A_{wire} produced by the piezos **142**, which produce the in-plane shear stresses S_x and S_y and help to dislodge the microbubbles **172** from the nucleation sites **130**, as discussed above. Flow boiling is enhanced within the microchannel **104** and, as a result, more of the cooling fluid **106** undergoes a phase change from liquid to vapor phase. The increase in vapor phase cooling fluid **106** produced within the microchannel **104** accounts for the increase in vapor pressure **176** measured by the absolute pressure transducer **178**. The fact that the top face temperatures remain close to saturated temperature is indicative of high HTC that corresponds to an effectively very thin time-average liquid film thickness (associated with Δt_{dwell} in FIG. **19**) wetting the boiling surface **126** while the RTD sensor probe remains, primarily, vapor blanketed (perhaps with even thinner liquid film coating the probe surface).

With reference to FIG. **10**, in another test, the microchannel **104** was likewise initially operated with the piezos **142** switched off. At about time=60 s, both piezos **142** were switched on. At about time=660 s, one piezo **142** was switched off while the other piezo **142** remained on. At about time=920 s, the remaining active piezo **142** was also switched off. As can be seen in FIG. **10**, a rapid increase in vapor pressure **176** was observed coinciding with activation of both of the piezos **142**, from about 105 kPa to about 125 kPa. Upon switching one of the piezos **142** off, the measured vapor pressure **176** decreased from about 125 kPa to about 115 kPa, but remained higher than the initial period when both piezos **142** were switched off.

With reference to FIG. **11**, multiple tests were conducted with the microchannel **104** with one or both of the piezos **142** switched on, and while varying the frequency and duty cycle of the piezos **142**. The results of these tests further demonstrate additional enhanced potentials and rapid increases in vapor pressure in response to activation of the piezos **142**. These pressure rises also correspond to significant HTC improvements in flow boiling performances relative to flow boiling performed without piezos but still employing the micro-structured boiling surface. Preliminary experimental results shown in FIG. **20** (which is a driving temperature difference versus average heat-flux plot) curves are quite reliable (within ±10-20% accuracy in driving temperature-differences) at heat-flux values in the immediate vicinity of 30 W/cm^2. The curves in this vicinity show an approximate HTC improvement of 132% for the micro-structured boiling surface case over the smooth plane copper case (which is at about 6277 W/m^2-° C.) and a further 287% HTC improvements for the piezos-actuated cases (reaching up to 56530 W/m^2-° C.) relative to the passive (no piezos actuation) meshed-copper case). While the trends of the extrapolated curves are not experimental, they are representative and are being established.

With reference to FIG. **20**, multiple tests were conducted with the microchannel **104** for a smooth boiling surface with the piezos **142** switched off, for the micro-structured boiling surface **126** with the piezos **142** switched off, for the micro-structured boiling surface **126** with the piezos **142** operating at a first setting, and for the micro-structured boiling surface **126** with the piezos **142** operating at a second setting. The results of these tests are provided by FIG. **20** and demonstrate that both the micro-structured boiling surface **126** and the piezos **142** improve the efficiency of the flow boiling process and yield higher heat transfer rates q at lower temperature differences ΔT.

With some modifications, the flow boiling approach utilizing micro-structuring and piezos-based enhancement of micro-nucleation rates as described above, can likewise significantly improve the performances of other pool-boiling based immersion cooling methods available in the market (e.g. from Iceotope, etc.).

FIG. **12** illustrates an exemplary cooling loop **200** that incorporates the cooling unit **100**. The cooling loop **200** is provided as an example of one implementation of the cooling unit **100**, but many other systems are possible for supplying, removing, and processing the cooling fluid **106** utilized by the cooling unit **100**. The exemplary cooling loop **200** includes a liquid-vapor mixer chamber **202**, a condenser **204**, a first pump **206**, a reservoir **208**, a second pump **210**, and a reheat apparatus **212**. Cooling fluid **106** exits the cooling unit **100** via the primary and secondary outlet ports **160**, **162** and flows to the liquid-vapor mixer chamber **202**. From the mixer chamber **202**, the cooling fluid **106** is drawn through the condenser **204** by the first pump **206**, and cooled to slightly below the saturation temperature of the cooling fluid **106**. The cooled cooling fluid **106** continues from the condenser **204** to the reservoir **208**. The second pump **210** draws the cooling fluid **106** from the reservoir **208** and directs it toward the cooling unit **100**. The second pump **210** also meters the flow rate of the cooling fluid **106** entering the cooling unit **100**, to maintain a steady state for the flow boiling process transpiring within the cooling unit **100**. The reheat apparatus **212** (e.g., a rope heater) is useful for cases where condenser exit sub-cooling becomes more than an allowed value. The reheat apparatus **212** reheats the cooling fluid **106** as necessary to ensure the cooling fluid **106** enters the cooling unit **100** at a temperature only slightly below the saturation temperature (e.g., 2-3° C. subcooled).

FIG. **13** schematically illustrates a server-level cooling subsystem **300** for cooling multiple microchips supported on

a server board **302**. The server-level cooling subsystem **300** employs multiple cooling units **100** to cool the microchips supported on the server board **302**. The server board **302** can be incorporated into a server rack **402** (FIG. **15**) which, in turn, can be utilized within a data center **702** (FIG. **17**) for performing various computing operations (e.g., machine learning applications, cloud computing, big data, internet of things, artificial intelligence, etc.). The server-level cooling subsystem **300** includes, in addition to the cooling units **100**, a server supply liquid line **304** for supplying cooling fluid **106** to the cooling units **100**. The server-level cooling subsystem **300** also includes a first or liquid server return line **306** for carrying away the (primarily liquid phase) cooling fluid **106** from the primary outlet ports **160** of the cooling units **100**. The server-level cooling subsystem **300** further includes a second or vapor server return line **308** for carrying away the (primarily vapor phase) cooling fluid **106** from the secondary outlet ports **162** of the cooling units **100**.

FIG. **14** schematically illustrates a rack-level cooling subsystem **400** for cooling multiple server boards **302** incorporated into the server rack **402**. The rack-level cooling subsystem **400** employs multiple server-level cooling subsystems **300** associated with multiple server boards **302**. For purposes of illustration, three server boards **302** are shown in FIG. **14**, but more server boards are also contemplated in accordance with well-known data center server rack configurations. The rack-level cooling subsystem **400** includes a supply manifold **404**, a first or liquid return manifold **406**, and a second or vapor return manifold **408**. A primary supply line **410** supplies liquid cooling fluid **106** to the supply manifold **404**, and multiple server liquid supply lines **304** extend between the supply manifold and each respective server-level cooling subsystem **300** to carry liquid cooling fluid **106** from the supply manifold **404** to each respective server-level cooling subsystem **300**. Multiple liquid server return lines **306** carry (at least partly) liquid phase cooling fluid **106** away from each server-level cooling subsystem **300** to the liquid return manifold **406**. The cooling fluid **106** exits the liquid return manifold **406** through a primary return line **412**. Similarly, multiple vapor server return lines **308** carry primarily vapor phase cooling fluid **106** away from each server-level cooling subsystem **300** to the vapor return manifold **408**. The cooling fluid **106** exits the vapor return manifold **408** through a secondary return line **414**.

FIG. **15** illustrates a server rack cooling loop **500** for circulating and removing heat from the cooling fluid **106** that flows through the server-level cooling subsystem **300** to cool the server rack **402**. In the illustrated embodiment, the server rack cooling loop **500** includes the server-level cooling subsystem **300** (employing multiple server-level cooling subsystems **300** each utilizing one or more cooling units **100**), and a cooling distribution unit (CDU) **502**. The CDU **502** receives heated and substantially vaporized cooling fluid **106** from the rack-level cooling subsystem **400** via the primary and secondary return lines **412**, **414** and supplies subcooled cooling fluid **106** to the rack-level cooling subsystem **400** via the primary supply line **410**. The CDU **502** includes a liquid-vapor mixer chamber **504**, a heat exchanger **506**, one or more pumps **508**, and a reheat apparatus **510** (for occasional use as necessary). A data center cooling line **512** is fluidly coupled to the heat exchanger **506** to carry away heat from the cooling fluid **106**. In some embodiments, the data center cooling line **512** is part of a heat recovery system **800** (FIGS. **17**, **18**A and **18**B) that is fluidly connected to the heat exchanger **506** (FIGS. **18**A and **18**B) to draw away heat from the cooling fluid **106**. The reheat apparatus **510** reheats the cooling fluid **106**, as necessary, to ensure that the cooling fluid **106** is supplied to the rack-level cooling subsystem at a temperature just below the saturation temperature.

FIG. **16** illustrates a block diagram of an exemplary control system **600** associated with the server rack cooling loop **500** that includes the cooling units **100**. The control system **600** includes a controller **150** that is electrically or otherwise communicatively connected to modules or components of the server rack cooling loop **500**. For example, the illustrated controller **150** is connected to pumps **508**, the reheat apparatus **510**, a power supply module **602**, a communications module **604**, and one or more cooling unit modules **606** associated with the cooling units **100**. Each cooling unit module **606** can include one or more temperature sensors **608** (e.g., the first temperature sensor **146**, the second temperature sensor **148**, the inlet temperature sensor **180**, etc.), one or more pressure sensors **610** (e.g., the absolute pressure transducer **178**, etc.), and the piezos **142**.

The controller **150** (FIG. **16**) can include any suitable combination of hardware and software that is operable to, among other things, control the operation of the server rack cooling loop **500** and the piezos **142**. The exemplary controller **150** includes a plurality of electrical and electronic components that provide power, operational control and, in some cases, protection to the components and modules within the controller **150** and/or the server rack cooling loop **500**. For example, the controller **150** can include, among other things, a processing unit **612** (e.g., a microprocessor, a microcontroller, or another suitable programmable device) and a memory **614**, and in some embodiments can be implemented partially or entirely on a semiconductor (e.g., a field-programmable gate array ("FPGA")) chip, such as a chip developed through a register transfer level ("RTL") design process.

The processing unit **612** can be connected to the memory **614** for execution of software instructions that are capable of being stored in the memory **614**. Software included in some implementations of the server rack cooling loop **500** can be stored in the memory **614** of the controller **150**. In some embodiments, the controller **150** is configured to retrieve from memory and execute, among other things, instructions related to the control processes and methods described herein. As will be appreciated, the controller **150** can include additional, fewer, or different components.

The illustrated communications module **604** is configured to connect to and communicate with other devices (e.g., a computer, a database, another server rack cooling loop, etc.) through a network **616**. The connections between the communications module **604** and the network **616** can be, for example, wired connections, wireless connections, or any combination of wireless and wired connections.

The controller **150** (FIG. **16**) receives temperature and pressure information from the temperature sensors **608** and the pressure sensors **610** of the cooling unit module **606**, and based on that information, executes instructions to maintain desired flow boiling parameters within the cooling units **100**. Specifically, the controller **150** can increase or decrease pump speeds of the pumps **508**, activate or deactivate the reheat apparatus **510**, and control operation of the piezos **142** as needed. The instructions can be pre-loaded to the controller **150**, or communicated to the controller via the communications module **604**.

As discussed above, the piezos **142** are excited to their natural frequency $f_p=(\Delta t_{piezo})^{-1}$ (about 1 MHz in the disclosed embodiment). To control the operation of the peizos **142**, the controller **150** imposes a tunable "on/off" modulation signal over the natural resonant signal at which the

piezos **142** are excited. The modulation signal produced by the controller **150** is a square wave having a period $\Delta t_{on}+\Delta t_{off}$ and a modulation frequency $f_M=(\Delta t_{on}+\Delta t_{off})^{-1}$. The on and off time periods Δt_{on} and Δt_{off} are adjusted by the controller **150** to tune the modulation frequency f_M and the energy associated with the modulation signal. The adjustments to Δt_{on} and Δt_{off} by the controller **150** determine the resultant acoustic waves A_{wire}, A_{cu}, and A_{fluid} generated by the piezos **142** and introduced into the microchannels **104**. As discussed above, the acoustic waves A_{wire}, A_{cu}, and A_{fluid} induce resonance with the "in-plane" natural frequencies of the micro-structured boiling surface **126**, frequencies associated with aggregate microbubble ebullition cycles on the boiling surface **126**, and suitable hydrodynamic acoustic force frequencies that act on the microbubbles when formed within the cooling fluid **106**.

The adjustments to Δt_{on} and Δt_{off} by the controller **150** are made in response to various input signals received from the sensors monitoring operation of the cooling unit **100** and the associated cooling loop **200**. For example, the inputs may include temperature and pressure information from the temperature sensors **608** and the pressure sensors **610** as discussed above, inlet and outlet mass flow rates, calculated average heat-flux impositions from the heat source **102**, inlet and outlet qualities of the cooling fluid **106**, etc., and any combinations thereof. Based on the feedback from the input signals, the controller **150** can execute instructions to perform the adjustments to Δt_{on} and At_{off} according to control methods generally known in the art (e.g., PID loop control techniques, machine learning processes, etc.), in order to achieve the desired enhanced flow boiling cooling results described above (as indicated by, e.g., the characteristic pressure rise inside the microchannels **104** discussed above).

FIG. **17** illustrates one configuration of a data center energy system **700** for providing power and thermal management to the data center **702**. The data center **702** implements the flow boiling server rack cooling systems described above. In the illustrated embodiment, the data center energy system **700** includes an on-site mini-combine cycle power plant (mini-CCPP) **704** provided locally at a site location of the data center **702** for generating electrical power supplied to the data center **702**. The mini-CCPP **704** includes micro gas turbines (MGTs) **706** to generate a primary supply of electrical power from a fuel source, and one or more organic Rankine Cycle turbines (ORCs) **708** to generate a secondary supply of electrical power from recovered thermal energy. The data center energy system **700** also includes a site substation **710** that receives electrical power from an energy grid **712**, and transformers **714** for transferring the electrical power from the site substation **710** and from the mini-CCPP **704** to the data center **702**. As shown in FIG. **17**, during periods of low power usage, the mini-CCPP **704** can also supply electrical power to the energy grid **712**. The data center energy system **700** also includes a heat recovery system **800** that recaptures thermal energy generated by the server racks **402**, and by the MGTs **706**. The heat recovery system **800** delivers the recovered thermal energy to the ORCs **708** to produce the secondary supply of electrical power (e.g., for recycled use in powering the data center **702**, or for returning to the energy grid **712**).

FIG. **18**A illustrates the heat recovery system **800** in further detail. For purposes of illustration, the heat recovery system **800** is shown coupled to a single server rack cooling loop **500** in FIG. **18**A, but the system **716** can be scaled to serve multiple server rack cooling loops **500** by means generally known in the art. The heat recovery system **800** includes a heat recovery vapor generator (HRVG) **802**, a condenser **804**, and a pump **806** in fluid communication with the ORC **708** and the heat exchanger **506** of the server rack cooling loop **500**. The heat recovery system **800** circulates an organic fluid (e.g., isopentane) within a closed heat recovery loop **808** that includes the HRVG **802**, the condenser **804**, the pump **806**, and the heat exchanger **506**. The HRVG **802** is further coupled to the MGTs **706** to receive exhaust gases therefrom. The HRVG **802** raises the heat recovery level by raising the "work potential" of the lower grade heat available from the data center **702**.

In operation, the heat recovery system **800** circulates the organic fluid through the closed heat recovery loop **808** by operation of the pump **806**. The organic fluid, in liquid phase, passes through the heat exchanger **506** and receives heat from the cooling fluid **106** circulating through the server rack cooling loop **500**. The organic fluid exits the heat exchanger **506** and passes through the HRVG **802**, where the organic fluid is further heated by the exhaust gases coming from the MGTs **706** and transitions to vapor phase. The vapor phase organic fluid then continues to the ORC **708**, which harvests energy from the organic fluid to generate the secondary electrical power supply. From the ORC **708**, the organic fluid passes to the condenser **804** and transitions back to liquid phase.

FIG. **18**B illustrates another embodiment of the heat recovery system **800**. In the embodiment of FIG. **18**B, the heat recovery system **800** further includes a battery stack **810** that stores electrical energy generated by the MGTs **706** and by the ORC **708**. The battery stack **810** selectively supplies electrical power to the data center **702**. In the embodiment of FIG. **18**B, the MGTs **706** are no longer the primary power supply—and the power supply is a mix of the battery stack **810**, the (relatively smaller in kWs) MGTs **706**, the ORC **708**, and a solar device **812** for partially charging the battery stack **810**. The heat recovery system of FIG. **18**B is also able to significantly reduce grid power consumption (thereby cutting operational costs), cut fossil fuel uses, and increase uses of renewables. In fact, depending on local needs and fuel availabilities, the small MGTs **706** in FIG. **18**B can be eliminated in some embodiments by replacing the HRVG **802** by a burner-fired HRVG version that can be procured through suitable vendors. The numerical values identified within FIGS. **18**A-**18**B are exemplary in nature and other values for other heat recovery systems **800** may be observed or designed for in other systems **800**.

The above disclosure uniquely enables chip to server to rack to data center level cooling and waste heat recovery as per discussions for illustrations in FIGS. **1**A-**20**. This leads to performance and economic superiority over the latest liquid cooling technologies (mostly using single-phase water) in the market.

Immersion cooling techniques (pool boiling based) utilized in the market are not discussed, but a person having ordinary skill in the art can readily apply and adapt microstructures and piezos enhanced flow-boiling approaches described herein to pool boiling systems and system components to significantly improve immersion cooling technologies as well.

In flow through the channels in flow-boiling, besides the boiling-surface process innovations discussed here, the flow is needed for two reasons: (i) liquid supply rate is needed to be greater than vapor generation rate, and (ii) both the vapor generated and surplus liquid need to be forced out of the exit of the channels. Pool boiling simply retains the boiling-surface process innovations discussed here and (i) the stagnant liquid pool automatically tunes liquid supply (by gravity) rate to be equal to the vapor generation rate at the

boiling-surface, as well as (ii) it automatically removes the vapor from the boiling-surface by upward buoyancy induced motions (with the vapor eventually being moved out of the reservoir's free-surface on to a condenser and then fed back into the reservoir). Therefore microstructures and piezos enhanced pool-boiling approach for immersion cooling is also contemplated herein.

The foregoing detailed description of the certain exemplary embodiments has been provided for the purpose of explaining the general principles and practical application, thereby enabling others skilled in the art to understand the disclosure for various embodiments and with various modifications as are suited to the particular use contemplated. This description is not necessarily intended to be exhaustive or to limit the disclosure to the exemplary embodiments disclosed. Any of the embodiments and/or elements disclosed herein may be combined with one another to form various additional embodiments not specifically disclosed. Accordingly, additional embodiments are possible and are intended to be encompassed within this specification and the scope of the appended claims. The specification describes specific examples to accomplish a more general goal that may be accomplished in another way.

As used in this application, the terms "front," "rear," "upper," "lower," "upwardly," "downwardly," and other orientational descriptors are intended to facilitate the description of the exemplary embodiments of the present disclosure, and are not intended to limit the structure of the exemplary embodiments of the present disclosure to any particular position or orientation. Terms of degree, such as "substantially" or "approximately" or "about" are understood by those of ordinary skill to refer to reasonable ranges outside of the given value, for example, general tolerances or resolutions associated with manufacturing, assembly, and use of the described embodiments and components.

Although the disclosure has been described in detail with reference to certain preferred embodiments, variations and modifications exist within the scope and spirit of one or more independent aspects of the disclosure as described.

Clause 1: a cooling module for an electronic device, the cooling module comprising: a body having formed therein a plurality of channels, each channel of the plurality of channels defined by a first channel surface and opposing lateral channel surfaces cooperatively defining a rectangular cross section normal to a channel axis; a micro-structured boiling surface positioned adjacent the first channel surface of each channel; a piezoelectric transducer in acoustic communication with one of the opposing lateral channel surfaces of each channel and configured to direct acoustic waves on the micro-structured boiling surface; an inlet header in fluid communication with each channel of the plurality of channels; and an outlet header in fluid communication with each channel of the plurality of channels.

Clause 2: the cooling module of clause 1, wherein the distance between opposing lateral channel surfaces of each channel is greater than 6 mm.

Clause 3: the cooling module of clause 1, wherein the micro-structured boiling surface is a micro-structured mesh.

Clause 4: the cooling module of clause 3, wherein the micro-structured mesh is formed from copper.

Clause 5: the cooling module of clause 1, wherein the piezoelectric transducer is a first piezoelectric transducer and including a second piezoelectric transducer in acoustic communication with the other opposing lateral channel surface.

Clause 6: the cooling module of clause 5, wherein the first and second piezoelectric transducers are transverse mode piezoelectric transducers having a resonant frequency f_p of about 1 megahertz (MHz).

Clause 7: The cooling module of clause 5, wherein the first and second piezoelectric transducers are transverse mode piezoelectric transducers having a resonant frequency (f_p), and further including a controller configured to provide a range of acoustic modulating frequencies (f_M) resulting from signals of modulating strengths available at f_p and $f_{p\pm}n\cdot f_M$ where "n≥1" is an integer.

Clause 8: the cooling module of clause 5, wherein the first and second piezoelectric transducers are configured, when a cooling fluid is flowing within the channel, to introduce acoustic waves sufficient to induce resonance of the micro-structured boiling surface.

Clause 9: the cooling module of clause 7, wherein the outlet header includes a primary outlet port and a secondary outlet port, the secondary outlet port configured to receive a liquid-vapor mixture of the cooling fluid.

Clause 10: the cooling module of clause 1, wherein the cooling module is mountable on a microchip for thermal communication therewith.

Clause 11: the cooling module of clause 1, wherein each channel has a length along the channel axis no greater than 6 cm.

Clause 12: a method of cooling an electronic device, the method comprising: passing a heat transfer fluid through one or more channels formed in a cooling module body, each channel defined by a first channel surface and lateral channel surfaces and further including a micro-structured boiling surface adjacent the first channel surface; and energizing a piezoelectric transducer in acoustic communication with one of the lateral channel surfaces of each channel to direct in plane acoustic waves on the micro-structured boiling surface and its vicinity to facilitate formation of microbubbles within the heat transfer fluid at microbubble nucleation sites on the micro-structured boiling surface.

Clause 13: the method of clause 12, wherein passing the heat transfer fluid through one or more channels means passing a subcooled heat transfer fluid through one or more channels.

Clause 14: the method of clause 13, wherein the subcooled heat transfer fluid is within 3° C. of its saturation temperature.

Clause 15: the method of clause 12, wherein energizing a piezoelectric transducer coupled to one of the lateral channel surfaces of each channel to direct in plane acoustic waves on the micro-structured boiling surface means energizing the piezoelectric transducer to its natural 1 MHz frequency (f_p) and thereafter imposing and tuning modulating frequencies (f_M) associated with an on-off mechanism of the controller resulting in acoustic energy in a modulating frequency range of 1-2000 Hz.

Clause 16: the method of clause 12, wherein energizing a piezoelectric transducer coupled to one of the lateral channel surfaces of each channel to direct acoustic waves toward the micro-structured boiling surface means energizing the piezoelectric transducer to a frequency of between 1 and 2000 Hz.

Clause 17: A controller for a server rack cooling loop for cooling a plurality of electronic devices, the controller comprising: a processor configured to receive inputs of a cooling loop temperature and pressure, determine desired flow boiling parameters of the cooling loop, and transmit signals to a piezoelectric transducer in acoustic communication with a flow channel of the cooling loop that is in

thermal communication with an electronic device, the signals configured to operate the piezoelectric transducer to resonate a micro-structured boiling surface positioned within the flow channel.

Various features of the disclosure are set forth in the following claims.

What is claimed is:

1. A cooling module for an electronic device, the cooling module comprising:

a body having formed therein a plurality of channels, each channel of the plurality of channels defined by a first channel surface positioned between opposing lateral channel surfaces to define a rectangular cross section normal to a channel axis;

a micro-structured boiling surface positioned adjacent the first channel surface of each channel;

a first piezoelectric transducer in acoustic communication with one of the opposing lateral channel surfaces of each channel and a second piezoelectric transducer in acoustic communication with the other opposing lateral channel surface, each transducer configured to direct acoustic waves on the micro-structured boiling surface;

an inlet header in fluid communication with each channel of the plurality of channels; and

an outlet header in fluid communication with each channel of the plurality of channels,

wherein the first and second piezoelectric transducers are transverse mode piezoelectric transducers having a resonant frequency (f_p), and further including a controller configured to provide a range of acoustic modulating frequencies (f_M) to the transducers resulting from signals of modulating strengths available at f_p and $f_{p\pm}n \cdot f_M$ where "n≥1" is an integer.

2. The cooling module of claim **1**, wherein a distance between the opposing lateral channel surfaces of each channel is greater than 6 mm.

3. The cooling module of claim **1**, wherein the micro-structured boiling surface is a micro-structured mesh.

4. The cooling module of claim **3**, wherein the micro-structured mesh is formed from copper.

5. The cooling module of claim **1**, wherein the first and second piezoelectric transducers are configured, when a cooling fluid is flowing within the channel, to introduce acoustic waves sufficient to induce resonance of the micro-structured boiling surface.

6. The cooling module of claim **1**, wherein the outlet header includes a primary outlet port and a secondary outlet port, the secondary outlet port configured to receive a liquid-vapor mixture of the cooling fluid.

7. The cooling module of claim **1**, wherein the cooling module is mountable on a microchip for thermal communication therewith.

8. The cooling module of claim **1**, wherein each channel has a length along the channel axis no greater than 6 cm.

9. A method of cooling an electronic device, the method comprising:

passing a heat transfer fluid through one or more channels formed in a cooling module body, each channel defined by a first channel surface and lateral channel surfaces and further including a micro-structured boiling surface adjacent the first channel surface; and

energizing a piezoelectric transducer in acoustic communication with one of the lateral channel surfaces of each channel to direct in plane acoustic waves on the micro-structured boiling surface and its vicinity to facilitate formation of microbubbles within the heat transfer fluid at microbubble nucleation sites on the micro-structured boiling surface,

wherein energizing the piezoelectric transducer in acoustic communication with one of the lateral channel surfaces of each channel to direct in plane acoustic waves on the micro-structured boiling surface means energizing the piezoelectric transducer to its natural 1 MHz frequency (f_p) and thereafter imposing and tuning modulating frequencies (f_M) associated with an on-off mechanism of the controller resulting in acoustic energy in a modulating frequency range of 1-2000 Hz.

10. The method of claim **9**, wherein passing the heat transfer fluid through one or more channels means passing a subcooled heat transfer fluid through the one or more channels.

11. The method of claim **10**, wherein the subcooled heat transfer fluid is within 3° C. of its saturation temperature.

* * * * *